FOI
SWEDISH DEFENCE
RESEARCH AGENCY

FOI-R--0771--SE
January 2002
1650-1942

Technical report

Anton Vooren

Expanding ADMIRE's Aerodynamic Envelope for High Angles of Attack

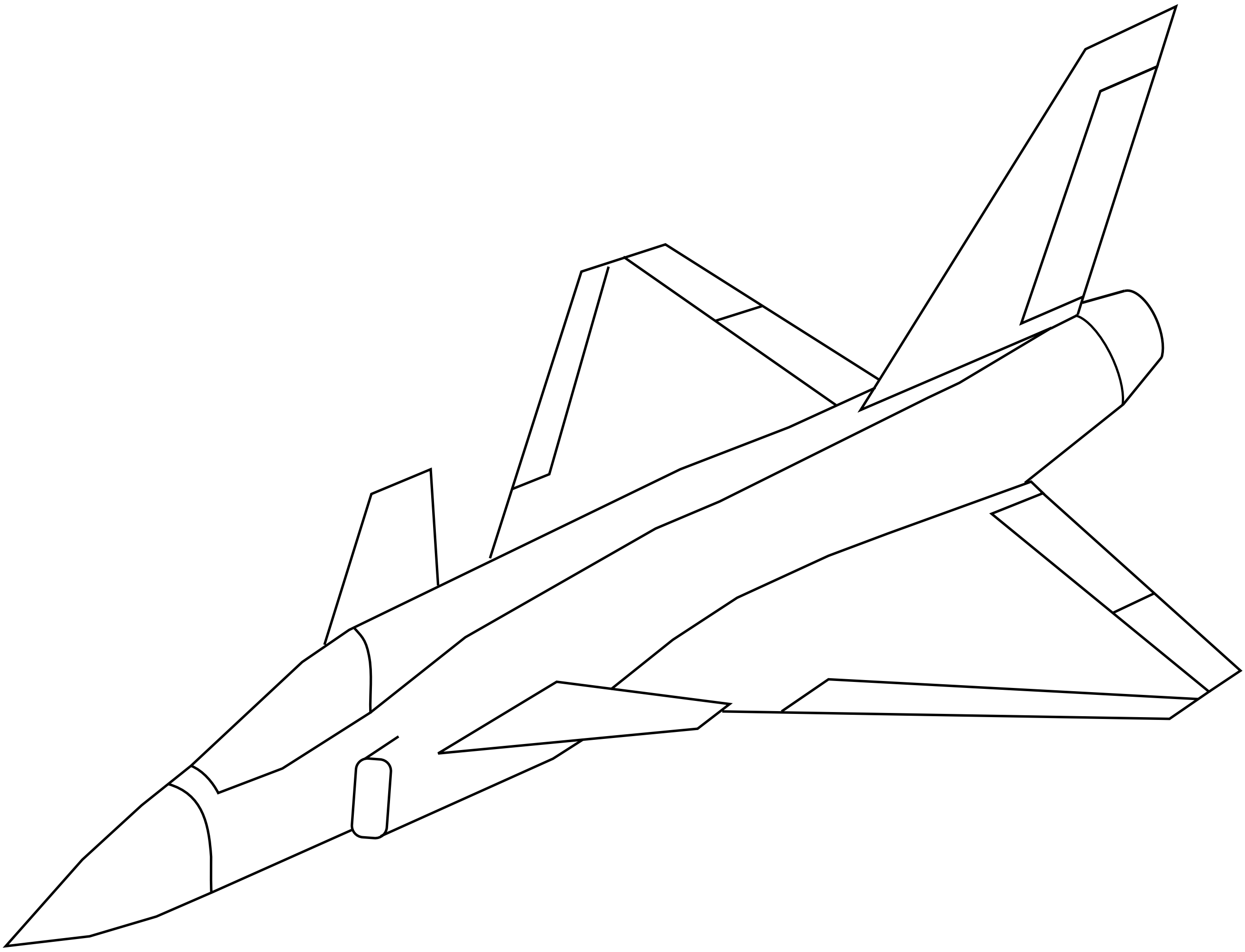

System Technology Division
SE-172 90 STOCKHOLM
Sweden

Swedish Defence Research Agency
System Technology Division
SE-172 90 STOCKHOLM
Sweden

FOI-R--0771--SE
January 2002
1650-1942

Technical report

Anton Vooren

Expanding ADMIRE's Aerodynamic Envelope for High Angles of Attack

Issuing organization	Report number, ISRN	Report type
Swedish Defence Research Agency System Technology Division SE-172 90 STOCKHOLM Sweden	FOI-R--0771--SE	Technical report
	Research area code: Vehicles	
	Month year: January 2002	Project no.: E6113
	Customers code: Aeronautical Research	
	Sub area code: Air Vehicles Technologies	
Author/s (editor/s): Anton Vooren	Project manager: Lars Forsell, Gunnar Hovmark	
	Approved by: Monica Dahlén	
	Sponsoring agency:	
	Scientifically and technically responsible: Lars Forsell, Gunnar Hovmark	

Report title

Expanding ADMIRE’s Aerodynamic Envelope for High Angles of Attack

Abstract

The aim of this report is to expand the aerodynamic database of an aircraft model called ADMIRE (Aero-Data Model In a Research Environment). The aircraft is a generic canard-delta configuration and the expansion has focused on it’s angle of attack range.
The new aerodynamic database is developed according to present theory on high angle of attack aerodynamic for close-coupled delta-canard configuration and compared with the X-31A aircraft. The angle of attack limit has been expanded from 30 degrees to 90 degrees and includes the effect of canard and elevon deflection. Fundamental increments of pitching moment, normal force and tangential force as functions of angle of attack have after the expansion been added to the original database.
The result is an aircraft with realistic controllability and behaviour at high angles of attack in longitudinal direction, but with unrealistic roll accelerations.
This report is a master’s thesis governed by the Department of Aeronautics at KTH and carried out on behalf of the Swedish Defence Research Agency.

Keywords

ADMIRE, high angle of attack, aoa, modelling, GAM, simulation, delta, canard, close coupled

Further bibliographic information	Language
	English
ISSN: 1650-1942	Pages: 57
Distribution: By sendlist	Price: Acc. to pricelist Security classification: Unclassified

Utgivare	Totalförsvarets forskningsinstitut Avdelningen för Systemteknik SE-172 90 STOCKHOLM Sweden
Rapportnummer, ISRN	FOI-R--0771--SE
Klassificering	Teknisk rapport
Forskningsområde	Farkoster
Månad, år	Januari 2002
Projektnummer	E6113
Verksamhetsgren	Flygteknisk forskning
Delområde	Flygfarkostteknik - övrigt
Författare/redaktör	Anton Vooren
Projektledare	Lars Forsell, Gunnar Hovmark
Godkänd av	Monica Dahlén
Uppdragsgivare/kundbeteckning	
Tekniskt och/eller vetenskapligt ansvarig	Lars Forsell, Gunnar Hovmark

Rapportens titel

Utvidning av ADMIREs Aerodynamiska Underlag för Höga Anfallsvinklar

Sammanfattning

Syftet bakom denna rapport är att utöka den aerodynamiska databasen för flygplansmodellen ADMIRE (Aero-Data Model In a Research Environment). Modellen beskriver en generisk delta-nosvingekonfiguration. Utvidgingen av enveloppen är fokuserad till anfallsvinkeln (α).
Den nya aerodynamiska databasen har utvecklats i enlighet med de senaste teoriena om hög-alfa aerodynamik för en så kallad "close-couplednosvinge-deltakonfiguration och har jämförts med databasen för X-31A. Modellens giltighet har ökats från 30° till 90° anfallsvinkel och inkluderar effekt från båda nosvingen och bakkantsrodren. Fundamentala bidrag till tippmomentet, normal- och tangential-kraften som funktion av anfallsvinkeln har inkorporerats i den ursprungliga databasen. Resultatet är en flygplansmodell med realistiska egenskaper och styrbarhet vid höga anfallsvinklar i longitudinell led, men med orealistiskt hög rollacceleration.
Detta arbetet har utförts som ett examensarbete på Institutionen för Flygteknik/KTH och har utförts vid Avdelningen för Systemteknik/FOI

Nyckelord	hög alfa, anfallsvinkel, GAM, ADMIRE, delta, canard
Övriga bibliografiska uppgifter	
Språk	Engelska
ISSN	1650-1942
Antal sidor	57
Distribution	Enligt missiv
Pris	Enligt prislista
Sekretess	Öppen

Contents

Symbols and Abbreviations

The symbols and abbreviations used in this report are listed below. In the bibliographed literature the use of symbols is not coherent, partly because of different configurations used. Most of the symbols are extracted from the GAM, see Backström [1], although sometimes modified to harmonize with common notation. The coefficients subscripts used in the GAM are left unaltered while symbols have been changed from FORTRAN variable names to textbook style notation (for example DEI $\longrightarrow \delta_{ei}$). The GAM's original abbreviations used in the aerodynamic tables can be seen in section A.3.

q_∞	Free stream dynamic pressure	N/m^2
$q_{a,corr}$	Non-dimensional $q_\infty \cdot \frac{1}{10000}$	
V_t	Aircraft velocity	m/s
M, M_∞	Mach number and free stream Mach number	
Re_C	Reynolds Number depending on mean aerodynamic chord	
h	Altitude	m
S_{ref}	Wing reference area	m^2
b_{ref}	Wing reference span	m
$\bar{c}_{ref}$	Mean aerodynamic chord	m
C_D	Drag coefficient	
C_d	Drag coefficient for a 2 dimensional body	
C_L	Lift coefficient	
C_N	Normal force coefficient	
C_T	Tangential force coefficient	
C_C	Side force coefficient	
C_m	Pitching moment coefficient	
C_l	Rolling moment coefficient	
C_n	Yawing moment coefficient	
$\bar{\delta}_e$	Mean elevon deflection (positive deflection downwards)	rad
δ_{ei}, δ_{ey}	Inner and outer elevon deflection (positive deflection downwards)	rad
$\bar{\delta}_n$	Mean canard deflection (positive deflection downwards)	rad
δ_{le}	Leading edge deflection (positive deflection upwards)	rad
δ_{ai}	Difference between inner elevon angle on either side	rad
δ_{ay}	Difference between outer elevon angle on either side	rad
δ_r	Rudder deflection (positive deflection right)	rad
cai	Engine mass flow ratio	
$eieff$	Aeroelastic effect on inner elevon	
$eoeff$	Aeroelastic effect on outer elevon	
α	Angle of attack (positive is nose up)	rad
$\dot{\alpha}$	Angle of attack rate	rad/s
β	Sideslip angle (positive is nose left)	rad
θ	Pitch attitude	rad
p, r, q	Roll, yaw and pitch rate (body fixed coordinate system)	rad/s
$\dot{p}, \dot{r}, \dot{q}$	Angular accelerations	rad/s^2
$\bar{p}, \bar{r}, \bar{q}$	Dimensionless angular velocity	
n_z	Load factor in body fixed frame of reference (B)	

Frames of Reference Used

The frames of reference used for this report are a body fixed frame of reference (F_B) and a frame of reference from which all coefficients are calculated (F_U). The frames of reference can be seen in Figure 1 where the arrows indicate positive direction. The body fixed frame of reference has its origin in the center of gravity (O_B). O_U is then placed with certain distance from O_B depending on for example aerodynamic center.

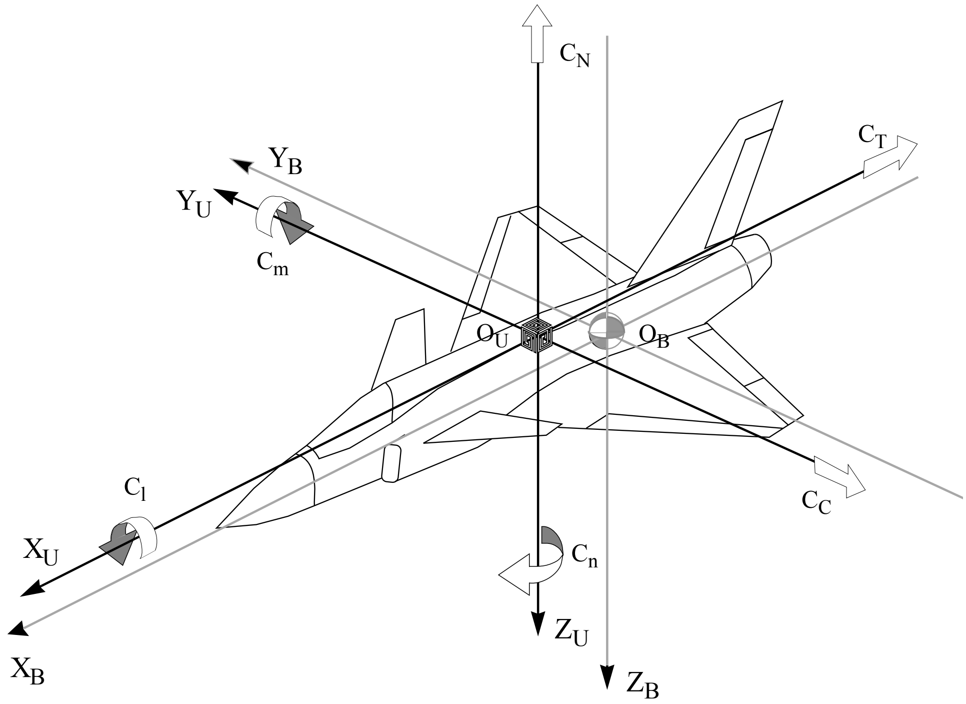

Figure 1: Body fixed frame of reference O_B and the aerodata frame of reference O_U

1. Introduction

The aim of this master's thesis is to expand the aerodynamic database of an existing aircraft model, to make an open model with a wide angle of attack range available.

In 1996 SAAB AB and KTH released an unclassified Generic Aero-data Model called GAM, see Backström [1]. The GAM was developed to have the complexity of a real aircraft model, and should for aerodynamic purposes be looked upon as a small single-seat, single engine fighter aircraft with a delta canard configuration.

Since the GAM is open and available for anyone interested, the Aeronautical Research Institute of Sweden (FFA), now merged with the Swedish Defence Research Establishment (FOA) to form the Swedish Defence Research Agency (FOI), has used it as an aerodynamic base in studies on aircraft modelling and control system design and testing. One application is the Aero-Data Model In a Research Environment called ADMIRE, see Forssell et al. [8], which has been used for research on the implementation of flight control system on complex aerodynamic data and for general simulations in the Flight Dynamics Simulator called FENIX[1].

During the flight simulator tests in the GARTEUR[2] AG-12 project regarding PIO[3], the runs were frequently aborted because the aircraft angle of attack and sideslip angle exceeded the limits in the aerodynamic database. If the limits had been wider, the excursions in pitch, yaw and roll could have been studied in a more realistic way. A wider angle of attack envelope would also be useful for tests with thrust vectoring and post-stall manoeuvres.

One problem is the lack of geometrical data. Except for reference data needed to calculate forces and moments, no other information about the GAM exist such as whether the canard is long or close-coupled and what the horizontal and vertical distances are between canard and wing. One alternative other than expanding the existing aerodynamic data, is to design a new virtual fighter and extract the aerodynamic data with the help of CFD[4]. This would, though, require much computer time and resources and does include risk of incorrect data and an aircraft with unpleasant characteristics. According to Bergmann and Hummel [5], considerable discrepancies occur between numerical and experimental data for higher angles of attack than 20 degrees.

Since the general configuration is known, like canard and delta wing, comparison can be made to similar fighters. Not many fighters have open sources though, but the aerodynamic data for the X-31A [3, 12, page 227-228] is open and has been used in this report.

The following report is a master's thesis at KTH with Professor Ulf Ringertz as examiner and has been executed at FOI with Lars Forssell and Gunnar Hovmark as supervisors. It is written for students at a masters degree level and requires basic knowledge in aerodynamics and stability. The ADMIRE is available at `http://www.foi.se/admire/` and the contact address is `mailto:admire@foi.se`.

1.1 Generic Aero-data Model (GAM)

The GAM is a delta canard fighter whose known measurements are in Table 1.1 except for reference values for control surfaces. No other open information about the geometry exists,

[1] see `http://www.foi.se/fenix/eng/`
[2] Group for Aeronautical Research and Technology in EURope
[3] Pilot Involved Oscillations
[4] Computational Fluid Dynamics

Component	Value	Unit
wing area (S_{ref})	45.00	m^2
canard area (S_c)	3.20	m^2
wing span (b_{ref})	10.00	m
canard span (b_c)	2.60	m
wing chord (mean) ($\bar{c}_{ref}$)	5.20	m
canard chord (c_c)	1.30	m
Mass (gross)	9100	kg
I_x	21000	kgm^2
I_y	81000	kgm^2
I_z	101000	kgm^2
I_{xz}	2500	kgm^2

Table 1.1: Nominal GAM configuration data as defined in ADMIRE

although a very general picture is shown in Figure 1.1. Compared to e.g JAS-39 Gripen [12, page 472-475], the GAM's wing area and span are bigger and the wing loading lower. The GAM's control surfaces consist of four wing trailing edge control surfaces, here called elevons, two wing leading edge control surfaces, here called leading edge flaps, one tail trailing edge control surface called rudder and a fully moveable canard (see Figure 1.1).

The GAM consists mainly of the aerodynamic data tables saved in SAAB's own "aer" format together with certain program routines. These are Fortran routines for summations of forces and moments, routines that look up the aerodynamic data and routines to make the linear interpolation in the aerodynamic tables.

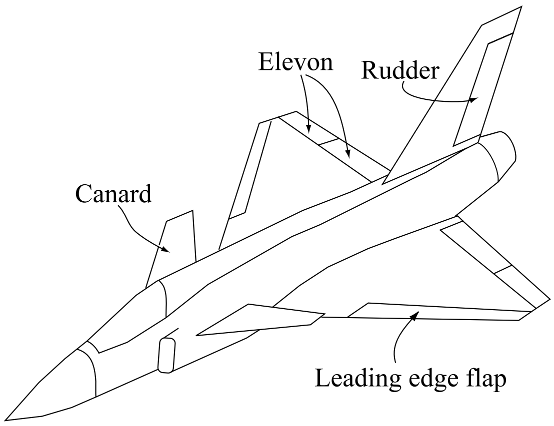

Figure 1.1: The GAM model as it is used for ADMIRE. The original SAAB picture (leading edge flap and engine differ) can be found in Backström [1] (aircraft is not to scale)

The GAM aerodynamic database is valid up to the Mach number 2.5. For Mach numbers below 0.4, the angle of attack range from $-10°$ up to $30°$ and the sideslip angle from $-20°$ to $20°$. Expanding the angle of attack range is for structural reasons only interesting in the low speed domain, which is below Mach 0.4.

To visualise the GAM's entire envelope, Figure 1.2 from Backström [1] has been included. The deflection of canard and elevon follows the right hand rule in a body fixed frame of reference. This implies that a positive deflection is when the trailing edge of the respective control surface moves down. The canard has a deflection of $-55°$ to $+25°$ and the elevon deflection range from $-30°$ to $+30°$. The leading edge has opposite signwise notation and it deflects from $-10°$ to $+30°$.

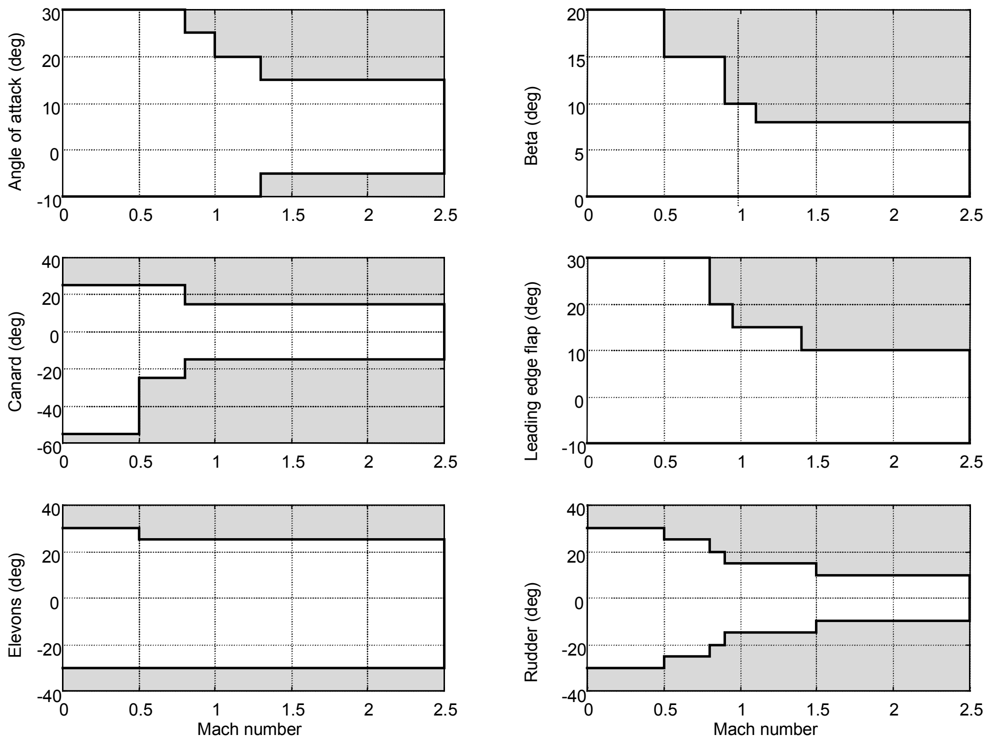

Figure 1.2: The GAM envelope

1.2 Aero-Data Model In Research Environment (ADMIRE)

ADMIRE (see Forssell et al. [8]) is an aircraft model with a flight control system and the GAM as its aerodynamic base. Most of the original Fortran routines have without significant changes been translated to C except for the aerodynamic table look-up routines that have been superseded by new and more effective C routines developed at FFA. An F-16 [11, page 640] engine has also been added together with a thrust-vectoring system. Since it was difficult to find the optimum settings for the leading edge flaps, these are fixed in ADMIRE at zero degrees.

In the rest of this report, the model will be referred to as ADMIRE, since there may be some differences between the GAM and ADMIRE characteristics caused for example by the different look-up and interpolation routines.

1.3 Acknowledgements

The author wishes to thank: FOI for allowing this project and specially the supervisor Gunnar Hovmark and Lars Forssell, Dag Wallström at FOI for valuable aerodynamic discussions and my beloved wife Carina for support and patience.

Credit for the occasionally good English language in this report should be given to Paul Morland and Gunnar Hovmark.

2. Methodology

2.1 Summary of Methodology

To be able to evaluate ADMIRE's existing data, the individual coefficients (see section A.3) have to be plotted for selected variables. Therefore MATLAB[1](see [14]) programs have been written where coefficient and variables can be individually chosen together with plot method. To evaluate these coefficients when added together, for example the aerodynamic longitudinal coefficients C_N, C_T and C_m, a copy of the Simulink[2] model of ADMIRE has been modified to exclude all non-stationary (dynamic) data. This way a wind tunnel measurement is simulated and comparable coefficients can be extracted.

Aerodynamic data from the X-31A are found to be suitable to a certain extent for comparison with ADMIRE. The X-31A data were scanned in from Reference [4] and plotted together with the output from the virtual wind tunnel. For every sweep in angle of attack from 30 to 90 degrees with constant control surface settings, a path of points is drawn. This path is based on the data from the X-31A together with present theory (see Chapter 3) and is later interpolated with a spline curve. The resulting curve is saved in steps of one degree between 30 and 90 degrees in the "aer" format. The new data tables are then implemented in the existing ADMIRE model and tested in the FOI simulator FENIX together with general tests in Simulink.

2.2 Extracting the Aerodynamic Data

To find the total aerodynamic data for the ADMIRE comparable to other aircraft, the coefficient parts shown in Appendix A have to be summed together at the preferred state (see example in Eq. 2.1).

$$C_T = C_{T_{basic}} + C_{T_{alpha}} + C_{T_{dei}} + C_{T_{dey}} + C_{T_{dedn}} + C_{T_{dn}} + C_{T_{dle}} + C_{T_{beta}} + C_{T_{da}} + C_{T_{dr}} \tag{2.1}$$

ADMIRE extracts data from the aerodynamic database for every new time step in the simulation and uses a linear interpolation function between the points in the database. The resultant coefficient is then used to find the static and dynamic behavior of the aircraft. If the dynamic part of ADMIRE is taken away, only the database look-up system and summation are left which is a suitable way of extracting the total static coefficients. The resulting simplified Simulink version of ADMIRE is implemented by Gunnar Hovmark, FOI, and called "ADMIRE Extract & Plot". Its Simulink scheme can be seen in Appendix C (time in this model is only used to stride through the states wanted). The input for the Simulink program is created in a MATLAB batch file that also extracts the result and plots it.

In contrast to the case in this report, total coefficient for most aircraft are found by using a wind tunnel. For example the well known C_L curve is easily found this way. With the method above, similar comparable static coefficients can be found.

2.3 Aerodynamic Data From Other aircraft

In the 80's, high angle of attack research had a high priority at several defence agencies. The need for highly manoeuvrable aircraft overtook the need for merely fast aircraft as experience

[1]MATLAB is a trademark of Mathworks and a language for technical mathematical computing

[2]Simulink is a trademark of Mathworks and is used for model-based and system-level design

indicated that both manoeuvrability and speed proved important for an aircraft's survivability. The values of these aircraft's aerodynamic coefficients cannot be used directly because of differences in geometry, but the tendencies can give a hint of how ADMIRE's aerodynamic coefficients should be extrapolated.

Several aircraft have been evaluated as possible candidates for comparison with the ADMIRE. The usable aerodynamic data available at FOI is limited to the HIRM, the F-16 and the F-18 (HARV) [2, 12, page 653] because of the open nature of the project. Most modern military aircraft developers are very secret about achieved data like EADS (Eurofighter 2000 [12, page 205-208]) and Mikoyan-Gourevitch (the MIG planes [12, page 392] besides the fact that there exists only a few unstable delta canard fighters. The most obvious source for aerodynamic data would be the Jas-39 Gripen [12, page 472-475] because of its origin, but this aircraft is unfortunately also classified.

Since ADMIRE is a canard delta aircraft with most likely a close-coupled canard, aircraft with the same characteristics are the most interesting. Only very few operative military aircraft are of this type. Table 2.1 shows the evaluated fighters and their relevance to this project. The MIG[3] fighter, Su fighters[4] and the Ye-8[5] are all Russian, the Rafale[6] is French, the JAS-39[7] Swedish, the Lavi[8] Israeli, the Eurofighter[9] and HIRM (only drop model) European while the rest are American[10]. The Russian fighters and the HIRM are all equipped with both canards and conventional tailplanes, and except for the MIG-1.42 MFI, their canards are very small.

Name	Company	Open source	Canard / Delta	Close-Coupled
F-16 Fighting Falcon	Lockheed Martin	$\alpha \to 45°$	No	N/a
F/A-18 HARV	McDonnel Douglas	$\alpha \to 90°$	No	N/a
HIRM	Garteur / DRA	$\alpha \to 120°$	Yes	No
X-31A EFM	Rockwell / DASA	$\alpha \to 67°$	Yes	No
Eurofighter 2000	EADS	No	Yes	No
Rafale	Dassault	No	Yes	Yes
MIG-1.42 MFI	MiG Corp. / MAPO	No	Yes	Yes
Su-32,-35	Sukhoi	No	Yes	Yes
Ye-8	MiG Corp. / MAPO	No	Yes	No
JAS-39 Gripen	SAAB	No	Yes	Yes
Lavi	Rafael	No	Yes	Yes

Table 2.1: Evaluated fighter aircraft

As seen from Table 2.1, only the X-31A and the HIRM are interesting and since the HIRM is a stable aircraft with very sparse data at high angles of attack, the X-31A is chosen to be the main source of aerodynamic data.

The X-31A is the most promising aircraft to compare with ADMIRE because of its similarity (canard and unstable), its amount of research data and because it has been used for high angle of attack research. It's however smaller and does have a long-coupled canard. The X-31A's coefficients are found in Banks et al. [4] and gathered in a MATLAB file to be compared with those from the ADMIRE. They were found to correlate enough to draw some conclusions. The geometry for the X-31A compared with the ADMIRE can be found

[3] See `http://www.aeroworldnet.com/1ra01189.htm` and `http://angela.ctrl-c.liu.se/misc/ram/i-42.html`

[4] See official homepage `http://www.sukhoi.org` and `http://angela.ctrl-c.liu.se/misc/ram/su-35.html`

[5] See `http://angela.ctrl-c.liu.se/misc/ram/ye-8.html`

[6] See `http://www.dassault-aviation.fr/defense/gb/Favionsarmes.cfm?ss_rubrique=rafale`

[7] See official homepage `http://www.gripen.saab.se`

[8] See `http://military.topcities.com/israel/lavi.htm`

[9] See `http://www.eurofighter.com/`

[10] See `http://military.topcities.com` or `http://www.fighter-planes.com`

Component	Value X-31A	ADMIRE	Unit
wing area	21.0	45.0	m^2
canard area	2.2	3.2	m^2
wing span	7.3	10.0	m
wing chord (mean)	3.7	5.2	m
Mass	7300	9100	kg
I_x	45700	21000	kgm^2
I_y	612000	81000	kgm^2
I_z	635000	101000	kgm^2

Table 2.2: Nominal X-31A and ADMIRE configuration data

in Table 2.2.

The coefficients available from the X-31A data set in Banks et al. [4] are three moments and three forces in the body fixed frame of reference together with C_L and C_D. The variables are canard, leading edge, elevon and rudder deflection together with speed brake and thrust vectoring. The exterior has also been changed during the test; particularly the nose, inlet and leading edge extension. The tables chosen are from the X-31A when it is configured with a flow through inlet, basic geometry nose, nose boom in its lowest position (N6), a strake of type S12 together with a basic type of leading edge without extension. The table for low angle of attack with neutral control surfaces is called "run 694" and for high angle of attack "run 670". Tables used for canard and elevon deflection are "run 668" through "run 674" together with "run 628" and "run 635". The canard deflection is denoted as δ_c and has a range from -60 degrees to 20 degrees. As a symbol for elevon deflection, $\delta_{f,TE}$ is used, which spans from -30 to 30 degrees. The X-31A leading edge deflection is denoted as $\delta_{f,LE}$.

No instationary effects are found in the X-31A data tables and no aeroelastic dependence or similar complicated data. Still, the huge difference in inertia between the X-31A and the ADMIRE indicate future differences in pitching moment and the influence magnitude from control surfaces. It can also be mentioned that the X-31A's ratio between main wing area and canard wing area is 9.5 which is to be compared to 14.0 for the ADMIRE. For that reason, the X-31A's canard can be more effective or, because of the long coupling between canard and wing, less effective than the ADMIRE's canard. The discrepancies between the X-31A and the ADMIRE will make the comparison harder.

2.4 Implementation

Since it has been impossible to extend all of the coefficient parts in Appendix A), only the most important inputs are extended for high angle of attack. For longitudinal motion the canard and elevon deflection are chosen. The resultant coefficients are divided into a main coefficient depending only on angle of attack and two parts depending on angle of attack and respective control surface deflection as seen in equation 2.2.

$$\begin{array}{l} C_N = C_N(\alpha) + \Delta C_N\left(\overline{\delta}_n, \alpha\right) + \Delta C_N\left(\overline{\delta}_e, \alpha\right) \\ C_T = C_T(\alpha) + \Delta C_T\left(\underline{\delta}_n, \alpha\right) + \Delta C_T\left(\underline{\delta}_e, \alpha\right) \\ C_m = C_m(\alpha) + \Delta C_m\left(\delta_n, \alpha\right) + \Delta C_m\left(\delta_e, \alpha\right) \end{array} \quad \text{, for } \alpha \in (30^\circ..90^\circ] \tag{2.2}$$

Since not all derivatives have been extended for the coefficients, it is likely to be differences in coefficient value when shifting from the original aerodynamic tables to the new ones for high angles of attack. One example is deployment of landing gear: The aircraft enters the extended envelope with landing gear retracted and extends it while angle of attack is above 30 degrees. This will give an increase in drag and change the moment curve, which is not covered in the extended envelope. Other examples are speed dependency and sideslip angle dependency.

To solve the blending of old and new coefficients, all coefficients depending on angle of attack keep as default their edge value when the aircraft is at an angle of attack of more than 30 degrees in ADMIRE. Therefore the new coefficients for high angles of attack are subtracted with the edge value and added as a difference as illustrated for the pitching moment coefficient C_m in Figure 2.1.

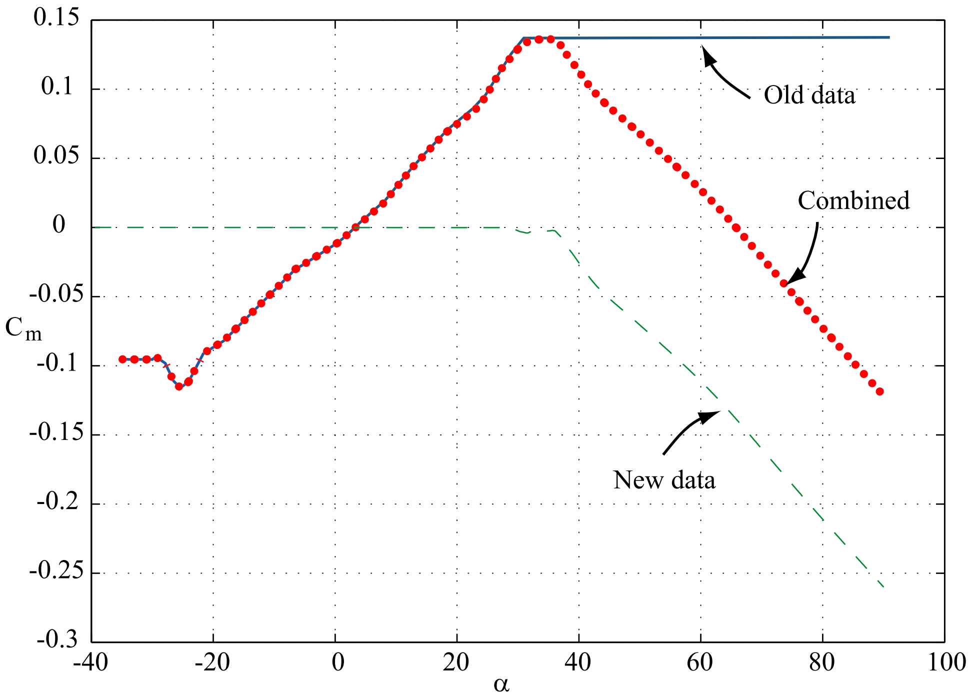

Figure 2.1: The original GAM $C_m(\alpha)$, the new high angle of attack increment and the combination of both

For the angle of attack dependent coefficient parts, the ones depending on angle of attack only and the ones depending on canard and elevon deflection will then change for angles of attack higher than 30 degrees. The rest of the angle of attack dependent coefficients will contribute with their edge value in the high angle of attack range.

Further implementations in ADMIRE not presented in this report consist of ADMIRE compilation and preparations for use in the real-time simulator FENIX, together with general changes needed in ADMIRE to include new aerodynamic data tables.

3. Theory

The ADMIRE aerodynamic characteristics for high angles of attack are governed by the interference between canard and wing vortices and their breakdown. In addition to these systems, the forebody vortices affect not only the canard and wing pressure coefficients but can for a missile body also create side forces (C_c) stronger than C_{Lmax} (Champigny [6]). The Institute of Fluid Mechanics at the Technical University in Braunschweig, Germany, has carried out much research on vortex issues and will be quoted extensively. General understanding about vortices can be gathered from Rom [15, Chap. 2,3,5,6]. The theory together with the aerodynamic data from similar aircraft will be the foundation for the new extended longitudinal ADMIRE database.

Vertical and horizontal canard distance with respect to main wing is not known for ADMIRE. From its original aerodynamic coefficients it can be seen that the derivative of C_L indicates stall after approximately 35 degrees. Stall is in this report defined as full canard and wing vortex breakdown. It occurs at a slightly higher angle of attack than $\alpha(C_{Lmax})$. Hummel and Oelker [10] have found that longitudinal positioning of canard within close-coupled domain gives a full stall around 35 degrees whilst the long-coupled canard system, on i.e. the X-31A, gives a full stall at 30 degrees.

The discussion above indicates that ADMIRE has a close-coupled canard and that will, according to Eugene [7], affect its aerodynamic characteristics. Together with the assumption about close-coupled canard, it will also be assumed a slender body and placement of canards and wings that ensure a good aerodynamic design without abrupt features.

In the following discussion, angle of attack is the wing, forebody or canard angle towards the free stream denoted α, the effective angle is the angle of attack that the surface really experiences in the near-flow field and the induced angle is the change in angle of attack because of an upwash or downwash field induced from another surface.

3.1 Vortex Systems on Slender Bodies

As already mentioned, three vortex systems are likely to appear at high angle of attack on a fighter with slender body, delta canard and delta wing. All three systems depend highly on geometry of which little is known. Still some qualitative conclusions can and will be drawn.

At angles of attack higher than approximately 5 degrees, vortices will start to form on both sides of the forebody. For higher angles of attack the theory is complex and is still a matter for discussion however this report will draw upon Champigny [6] and Stavöstrand [16]. As long as the vortex system is stable, the vortices will ensure high-energy flow over the canard and to some extent over the wings. Their breakdown will with increasing angle of attack travel forward to the vortex origin, and most likely become asymmetric before they disappear (i.e. go from unstable symmetric flow to stable asymmetric flow).

The asymmetric tendencies for fighter slender bodies seem to start at around 30 degrees angle of attack and end around 60 degrees. Also, it does not seem to occur at Mach numbers above 1.15. What triggers this behaviour is still not agreed on, but one explanation is that this happens because the two contrarotating vortices become strong and are very close to each other so that a small sideslip angle or perturbation will make one of the vortices stronger and suppress the other. Both vortices create a suction force on the side of the body and will therefore create a yawing moment when asymmetric. The result of the yawing moment will include some sideslip angle which will shadow the strong vortex and support the suppressed vortex to grow strong again with a side force of opposite magnitude as result. An illustrative figure can be seen in Stavöstrand [16, Fig. 3]. The asymmetric behavior can be of damping or accelerating nature throughout the alpha domain where it appears. The secondary effect is that the extra lift on canards and wings will vary together with the asymmetric pulsing of vortices which create a rolling moment sometimes called "wing ock". The canard vortex system formation is the same as on a delta wing according to Bergmann and Hummel [5]. The primary vortex will start in the intersection between canard leading edge and fuselage, followed by a secondary vortex travelling on the underside which together will be merged with the trailing edge vortex and travel towards the wing. Depending on the vertical position of the canard with respect to the wing, the canard vortex system will interact with the flow over the wing containing wing and fuselage vortices. (An illustrative picture made by Tuncer et al. [17, Figure 7] can be found in Figure 3.1.)

The wing vortex system develops in much the same way as the canard vortex system, but will be influenced by the canard vortices. This vortex system can also be seen in Figure 3.1. The wing vortex system tends to push the canard as well as fuselage vortex system (the last one not shown in figure) against the root of the wing. The wing vortex build up will be delayed because of the canard vortex system suppressing flow separation at the wing leading edge. In addition, the downwash of the canard gives the wing a lower effective angle (the sum of angle of attack and angle of canard downwash field).

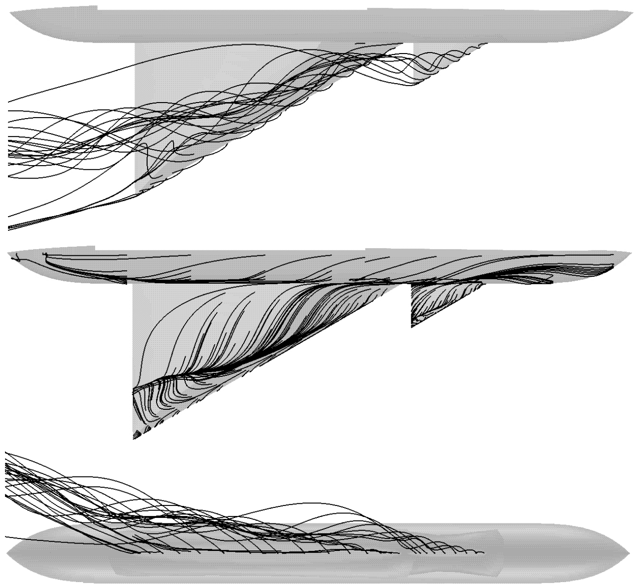

Figure 3.1: Computed turbulent flow over a delta canard configuration at $\alpha = 20^\circ,\ M_\infty = 0.2$ and $Re_C = 0.32 \cdot 10^6$. Fuselage vortex is not shown.

When angle of attack is higher than 35 degrees, full stall can (as described above) be assumed for a canard delta configuration. The flow field behind wing and canard will then have the characteristics of a wake. As mentioned above, some stable asymmetric vortices from the forebody can appear, flowing like a Karman gate and cause lift on either wing to vary dramatically with time.

3.2 Mutual Influence

The forebody will for all positive angles of attack create an upwash field which again will give the canard an induced angle of attack. The wing also has this effect on a close-coupled canard because it creates an upward flow around the wing leading edge and therefore an upwash flow field in front of the wing where the canard is placed. This implies that the canard effective angle of attack is higher than α and the canard will therefore stall at an α less than 35 degrees.

From Figure 3.2 it can be seen that $\bar{\delta}_n = 5^\circ$ and $\alpha = 0^\circ \Rightarrow C_m(\bar{\delta}_n, \alpha) \approx 0$. To keep the moment zero for even higher angle of attack, approximately the same effective canard angle of attack is required. Another look at Figure 3.2 shows that zero pitching moment at 30 degrees angle of attack requires -30° canard deflection which, when compared to $C_m(\bar{\delta} = 0, \alpha = 0^\circ)$ indicates an upwash from the forebody of 5°. These results can be used to predict $C_m = 0$ for higher angle of attack . Another result is that the point where the canard does more harm than good is in the upper right side of Figure 3.2 when pitching moment C_m decreases for increasing canard deflection (No explanation will be given for the phenomena occurring when $\alpha \in [-10^\circ..0^\circ]$ and $\bar{\delta}_n \in [0^\circ..-55^\circ]$). The reason for the steep increase in C_m even after the canard has stalled, is probably because of vortex breakdown at wing trailing edge that moves the aerodynamic centre forward and gives an increased nose up moment C_m.

Generally, every control surface deflection will cause increased drag. The effect from the canard on the normal force is the extra lift created. This is seen as an increase in lift for decreasing canard deflections until canard stall. An increasing tangential force is seen for all positive or negative lift-creating canard angles. The negative tangential forces are believed to originate from the so called nose-suction produced by the wing. Nose-suction varies with the lift produced, which is to say that this effect should decrease when the wing stalls. After stall, the tangential force should approach zero for every canard and elevon setting when angle of attack is approaching 90 degrees.

High angle of attack will also lead to loss in elevon effectiveness due to the change in flow at the wing trailing edge. This leads to less controllability in pitch and roll. Principally, a positive deflection of elevons will give a wing with increased lift and consequently drag. Depending on the center of gravity position in respect to the aerodynamic center, the increased lift and drag will cause a pitching moment C_m of some degree.

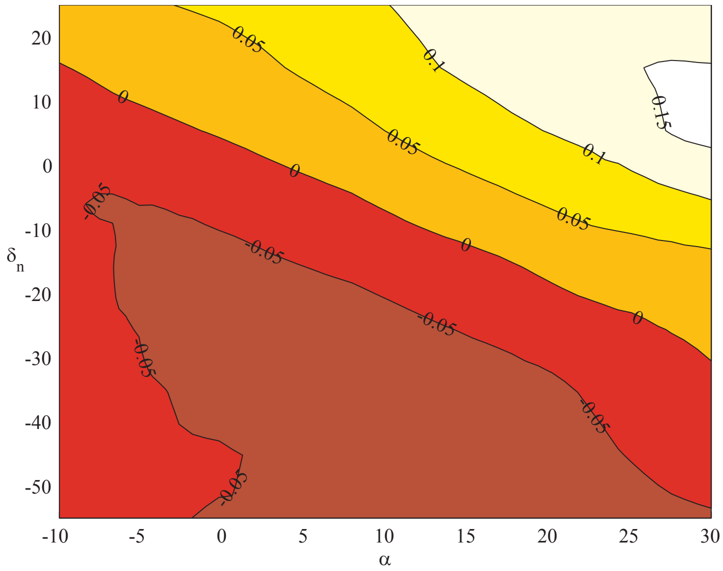

Figure 3.2: Contour plot of coefficient $C_m(\bar{\delta}_n, \alpha)$ extracted from the original GAM database

3.3 Known Points at 90 Degree Angle of Attack

An aircraft flying level with zero angle of attack will have $C_N = C_L$ and $C_T = C_D$. When an aircraft has an angle of attack of 90 degrees, $C_L = C_T \approx 0$ (see Equation 3.1 and 3.4). It can also be assumed that $C_N \approx C_D$ when the angle of attack is 90 degrees (see Equation 3.3) and that it is roughly the same as the aircraft's maximum drag at a given speed.

$$\begin{aligned}
C_L &= C_N \cdot cos(\alpha) - C_T \cdot sin(\alpha) && (3.1)\\
C_D &= C_N \cdot sin(\alpha) + C_T \cdot cos(\alpha) && (3.2)\\
&\Downarrow \\
C_N\,(\alpha = 90^\circ) &= C_D\,(\alpha = 90^\circ) && (3.3)\\
C_T\,(\alpha = 90^\circ) &= C_L\,(\alpha = 90^\circ) \approx 0 && (3.4)
\end{aligned}$$

If the normal force for a cylinder with an ogive nose is scaled to have same $C_N\,(\alpha = 90^\circ)$ as a fighter with a delta canard configuration, their normal and tangential force coefficient will in theory look like in Figure 3.3. In this Figure, the cylinder plot has been derived from Jorgensen [13].

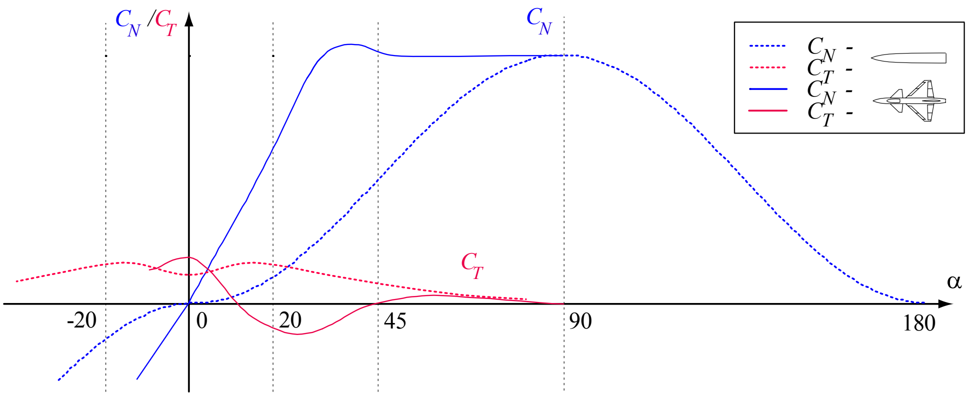

Figure 3.3: Coefficient $C_N\,(\alpha)$ and $C_T\,(\alpha)$ for a delta canard and a cylinder with ogive nose

Although C_N or C_D at $\alpha = 90^\circ$ are not so easy to calculate, a rough estimate can be readily established. If a few measures are guessed, like the area of the underside between the canards being equal to 2 m^2, then the total area that can be predicted as a plate is 50 m^2 (see Table 1.1). The nose (and engine exhaust) can be predicted as having a square cross section with rounded corners. According to Jorgensen [13, Table 1] given a high Reynolds number, a square cross section with rounded corners where radius is half the width, has a $C_d \approx 1.2$. Estimating this to be valid for the ADMIRE 3D body will give a $C_D \approx 1.2$. For a flat plate, Hoerner [9] estimates drag to be $C_D = 1.7$. This leads to Equation 3.5 and the maximum C_D. It is important to state that the wing is not a flat plate because some kind of profile is used. Therefore this estimation is probably too high and should be used accordingly.

$$\begin{aligned}
C_N\,(\alpha = 90^\circ) &= \frac{C_{plate} \cdot (S_{wing} + S_{canard} + S_{underside}) + C_{square} \cdot S_{nose}}{S_{ref}} \\
&= \frac{1.7 \cdot 50 + 1.2 \cdot 4}{45} \approx \underline{2.0}
\end{aligned} \qquad (3.5)$$

Besides the gravitation which can be counteracted with engine force, no force will have its direction across the airstream when angle of attack is 90°. This implies as stated in Equation 3.4 that C_T has to be zero.

For the pitching moment C_m only the slope sign can be foreseen. When the vortex system break down and stall occurs, the aircraft's center of pressure will move to the rear such that the aircraft in fact becomes stable while pitching moment is still positive. This implies a risk of being stuck in a stalled condition. If the aircraft's control surfaces cannot give enough change in pitching moment after stall, the danger exists of the aircraft becoming held in a for example "deep" stall. The aerodynamic should therefore be chosen carefully to prevent this from happening.

4. Results

The results will be presented in the form of plots with general comments. The actual data has been included in Appendix B. A reminder has to be given about the different reference area and mean chord between the ADMIRE and the X-31A as well as the long/close-coupled canard difference mentioned in the Theory chapter. This will give relatively prominent discrepancies and is why only the *tendencies* from the X-31A aerodynamic data should be counted on. MATLAB is not able to create a bar over the variables, so in the figures $\delta_n = \bar{\delta}_n$ *and* $\delta_e = \bar{\delta}_e$

4.1 Basic Coefficients

When all control surfaces are set neutral, a sweep in a wind tunnel will give very typical coefficient curves which to some extent can be compared to other aircraft. Figure 4.4, 4.1 and 4.2 show the ADMIRE coefficients below 30° together with the X-31A data for both below and above 30° overlapping each other. The new extrapolated data for the ADMIRE is marked as black crosses and can be seen overlapping the old data from 24° to 30° in order to give the spline function mentioned in Methodology a good derivate to start with.

As seen in Figure 4.1, a smooth stall has been chosen for the ADMIRE. The X-31A has a little more abrupt stall which is mainly due to the long-coupled canard. C_N follows the theoretical C_N in Figure 3.3 and the resulting C_L calculated with Equation 3.1 can be seen in Figure 4.3 where the point of vortex breakdown or stall is easier to see.

According to the theoretical C_T from Figure 3.3, the tangential force should move towards zero when the angle of attack increases beyond 40 degrees angle of attack. This is certainly not the case with the X-31A tangential force which seems to decrease for higher angle of attack. Negative tangential force is mostly referred to as nose-suction which is likely to be small on a stalled wing. Since C_T relative to C_N is very small in this region, no further evaluation has been done and a likely path has been chosen as drawn in Figure 4.2.

The result of the normal force and tangential force in the U frame of reference (see section "Frames of reference used") and Equation 3.1 and 3.2) is called C_L and C_D and has been included for the reader's convenience in Figure 4.3. Compared to conventional aircraft, the shift from positive to negative lift slope is much smoother and gives a less abrupt stall characteristic typical for canard equipped aircraft.

For a canard delta configuration, vortex breakdown at high angle of attack will shift the center of pressure rear of the center of gravity and the aircraft will become stable as explained in the Theory chapter. This is seen as a negative pitching moment C_m slope in Figure 4.4.

The chosen degree of the slope for both pitching moment C_m and normal force C_N has also drawn upon Stavöstrand [16, Fig. 1].

4.2 Canard dependency

For the sake of clearness, the three dimensional plots are not represented with both X-31A and ADMIRE coefficient data. Since this report probably will be read from a gray scale printout, effort has been made to use a color map that will be clear in both color and gray scale. The mean canard deflection $\bar{\delta}_n$ has been used since differences between left and right canard deflection should have little impact on the longitudinal characteristics.

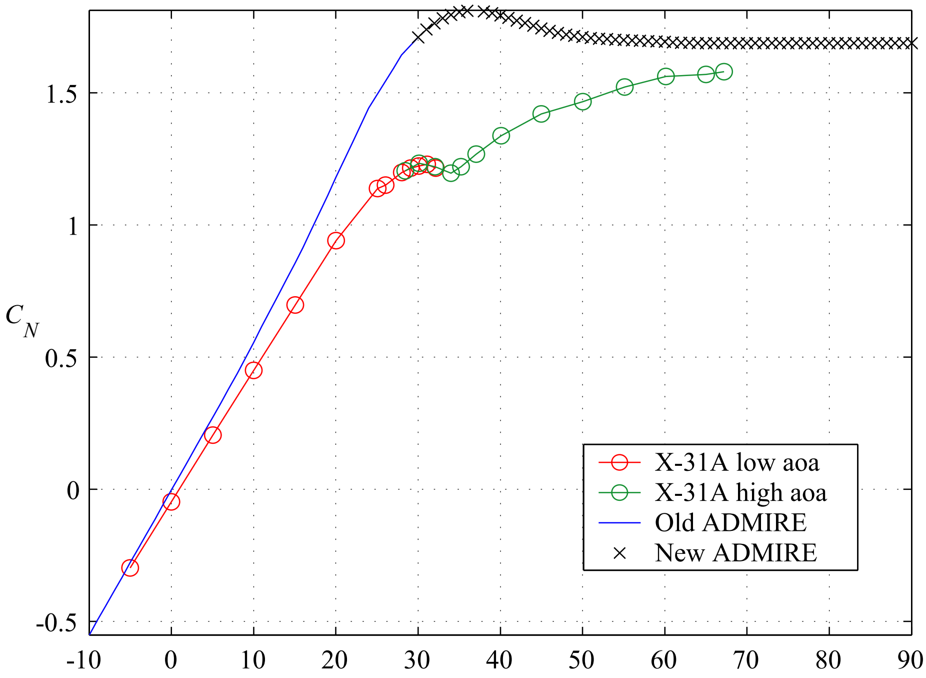

Figure 4.1: Coefficient $C_N(\alpha)$ with all control surfaces fixed in neutral position

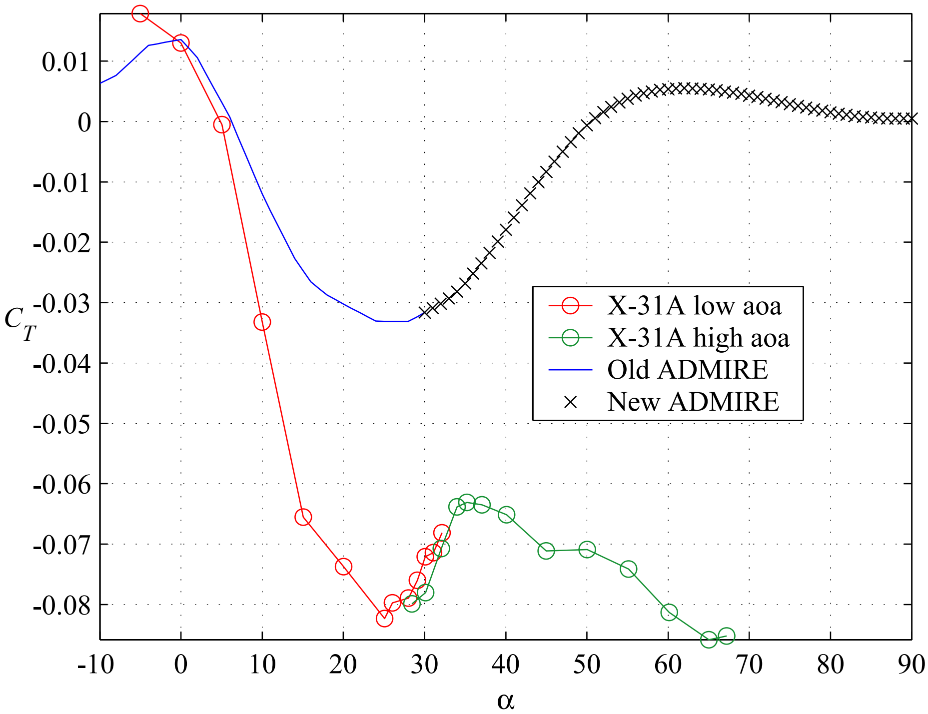

Figure 4.2: Coefficient $C_T(\alpha)$ with all control surfaces fixed in neutral position

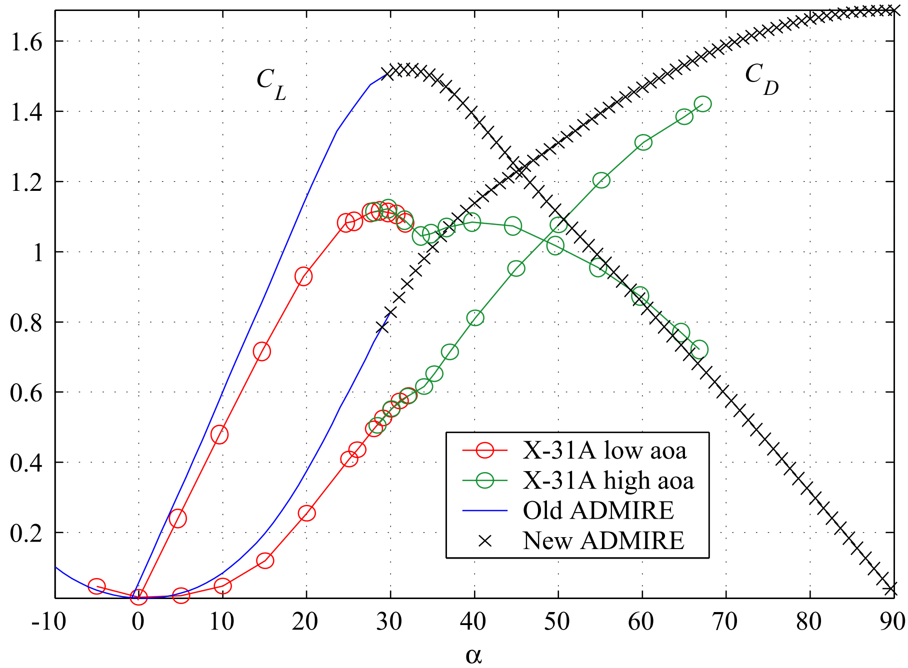

Figure 4.3: Coefficient $C_L(\alpha)$ and $C_D(\alpha)$ with all control surfaces fixed in neutral position

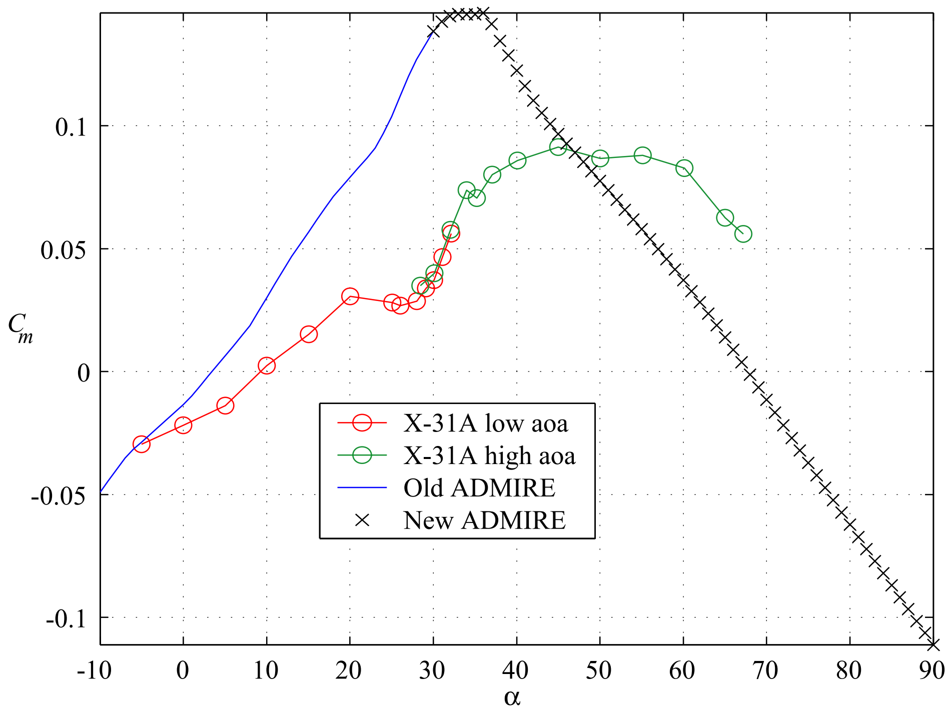

Figure 4.4: Coefficient $C_m(\alpha)$ with all control surfaces fixed in neutral position

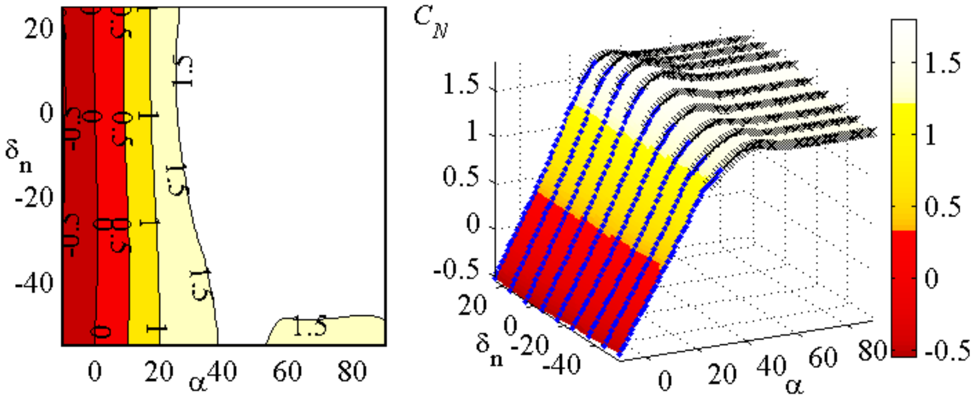

Figure 4.5: Contour (left) and 3D (right) plot of coefficient $C_N(\alpha, \bar{\delta}_n)$

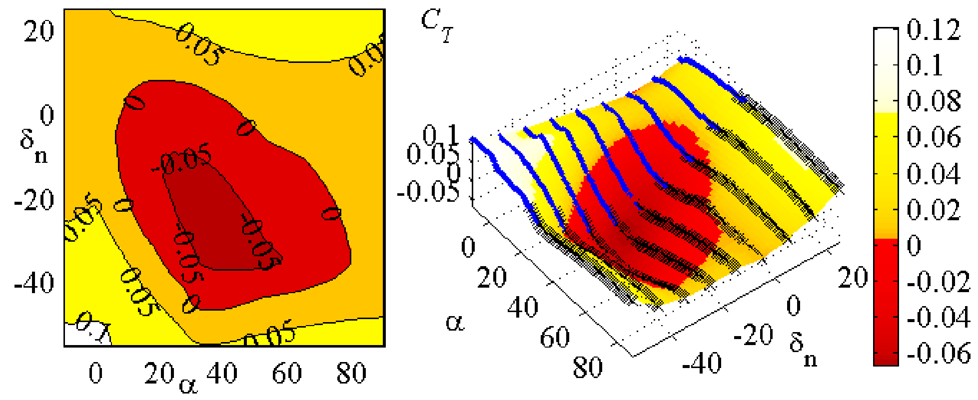

Figure 4.6: Contour (left) and 3D (right) plot of coefficient $C_T(\alpha, \bar{\delta}_n)$

Generally for both canard and elevon longitudinal dependency a characteristic has been chosen that should avoid any erratic behavior with today's control system.

Figure 4.5 shows how the normal coefficient C_N is chosen to change with respect to angle of attack and mean canard deflection. First of all maximum lift is where both canard and wing still generate positive lift which has to be at approximately the same angle of attack. From the basic lift curve in Figure 4.3, the wing will have its maximum lift at 32° angle of attack. Assuming an upwash from the forebody in front of the canard, a stall will appear earlier on the canard than on the wing. Therefore a peak can be expected around 35° angle of attack and $-5°$ canard deflection. From this peak the normal force will decrease for both positive and negative canard deflections. This tendency is expected to be less as the flow turns into a wake and will eventually be almost the same for every canard deflection when angle of attack is approaching 90°.

The canards contribution to drag has its minimum when the canard effective angle of attack is zero. For higher angles of attack the canard deflection impact on the tangential force will, as described above, decrease and move towards zero for 90 degree angle of attack and all canard deflections. The tangential force has been plotted in Figure 4.6

For the readers convenience, plots of the resulting drag and lift have also been included, see Figure 4.7 and 4.8.

Pitching moment C_m has been formed after canard stall behavior shown in Figure 4.9. The old GAM aerodynamic data indicate the highest pitching moment to be around 5 degrees canard angle. For higher canard angles, stall occurs and with that a shift in slope sign. For negative canard angles, the slope has been decreased and becomes negative after canard stall.

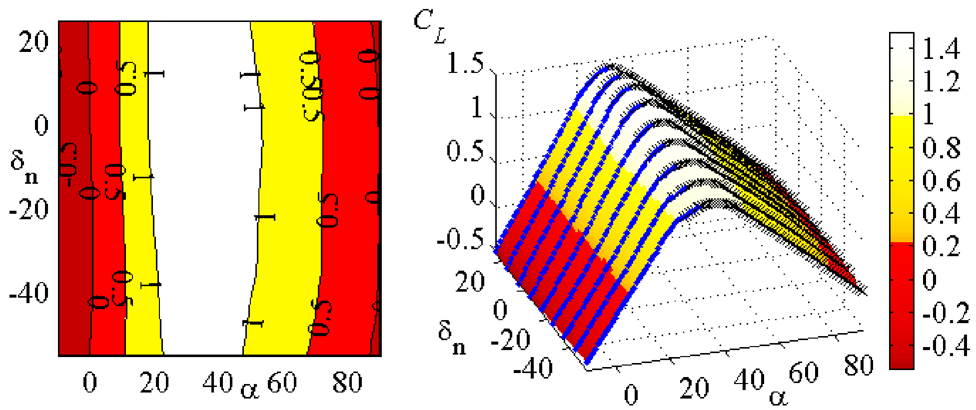

Figure 4.7: Contour (left) and 3D (right) plot of coefficient $C_L(\alpha, \bar{\delta}_n)$

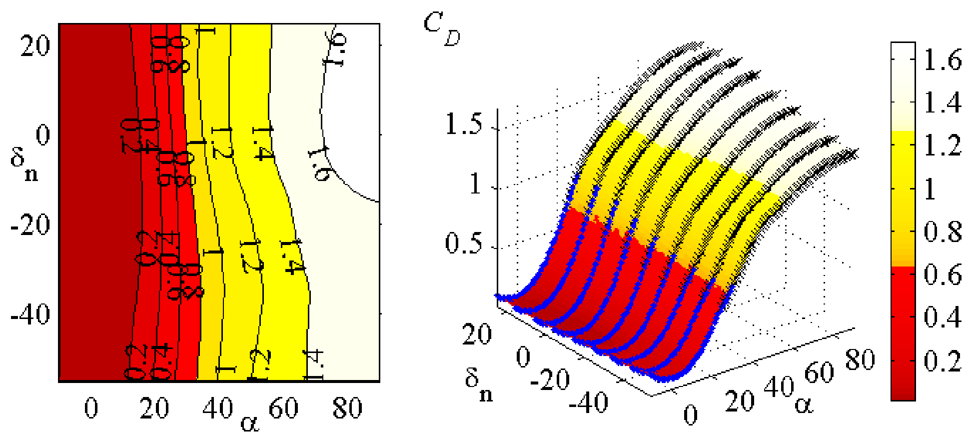

Figure 4.8: Contour (left) and 3D (right) plot of coefficient $C_D(\alpha, \bar{\delta}_n)$

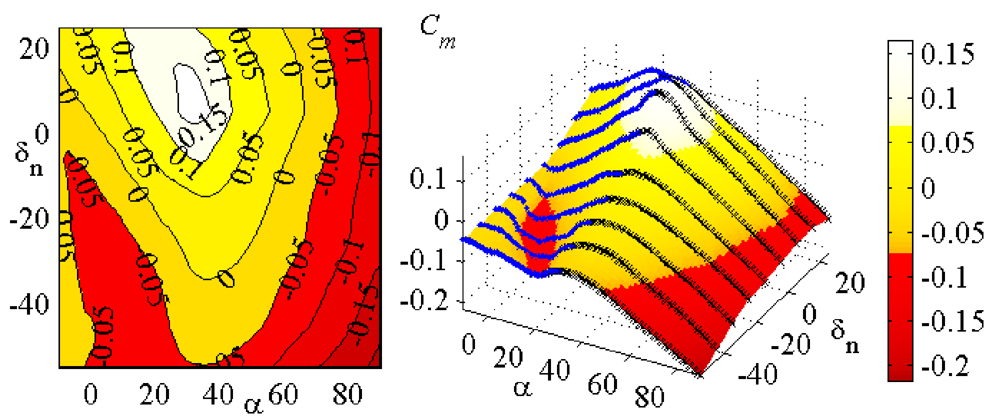

Figure 4.9: Contour (left) and 3D (right) plot of coefficient $C_m(\alpha, \bar{\delta}_n)$

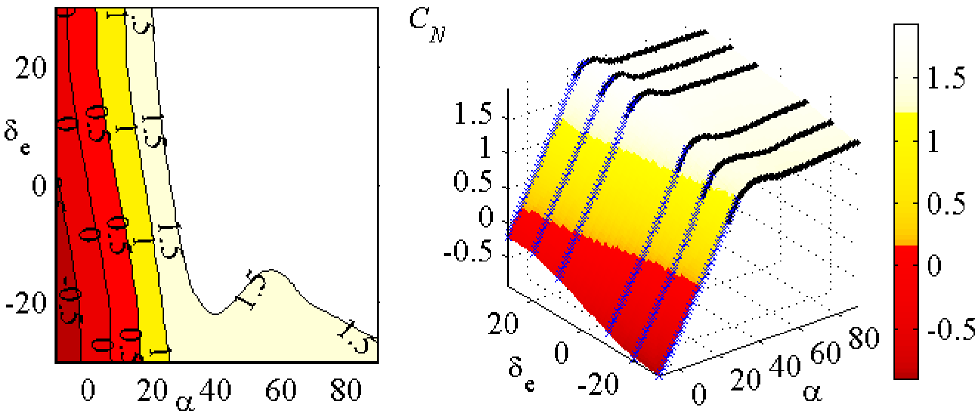

Figure 4.10: Contour (left) and 3D (right) plot of coefficient $C_N(\alpha, \overline{\delta}_e)$

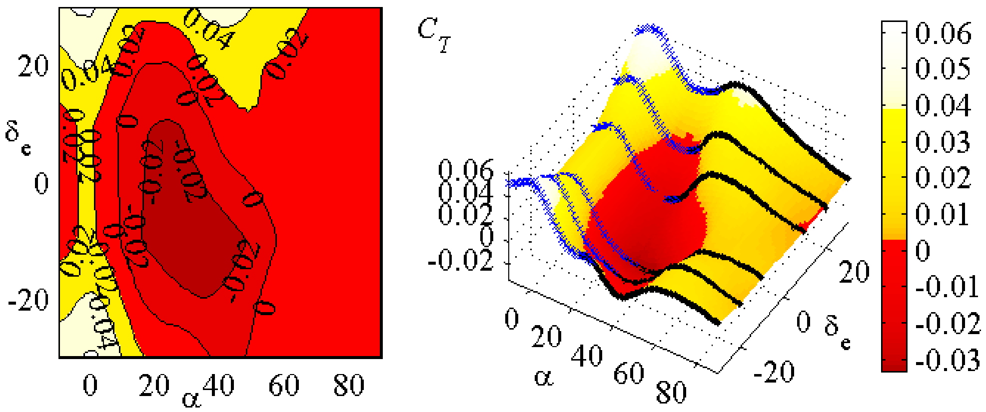

Figure 4.11: Contour (left) and 3D (right) plot of coefficient $C_T(\alpha, \overline{\delta}_e)$

4.3 Elevon dependency

An increasing elevon deflection will give a wing with increased lift as long as flow is attached to the wing. For an angle of attack below 25° and elevon deflections between $-20°$ and 20°, the normal force seems to be almost linearly dependent on elevon deflection as seen in Figure 4.10. For increasingly higher angle of attack, stall angle will depend on elevon deflection. A positive deflection gives earlier stall in terms of angle of attack than a negative deflection. A negative elevon deflection can postpone stall because the wing's effective angle of attack will decrease.

Figure 4.11 shows that when the ADMIRE has an angle of attack below stall angle, elevon impact on tangential force is almost symmetric around zero deflection. After stall, positive deflection will increase the tangential force while a negative deflection will have very little effect.

The effect of elevon deflection on lift C_L and drag C_D has been included, see Figure 4.12 and 4.13

Since the center of pressure over the wing will shift with elevon deflection, the pitching moment C_m generally will decrease with increasing elevon deflection. In Figure 4.14 the C_m dependency on elevon and angle of attack can be seen. Compared to the C_m dependency on canard deflection, the elevon has almost double impact on C_m (see Figure 4.9 and 4.14).

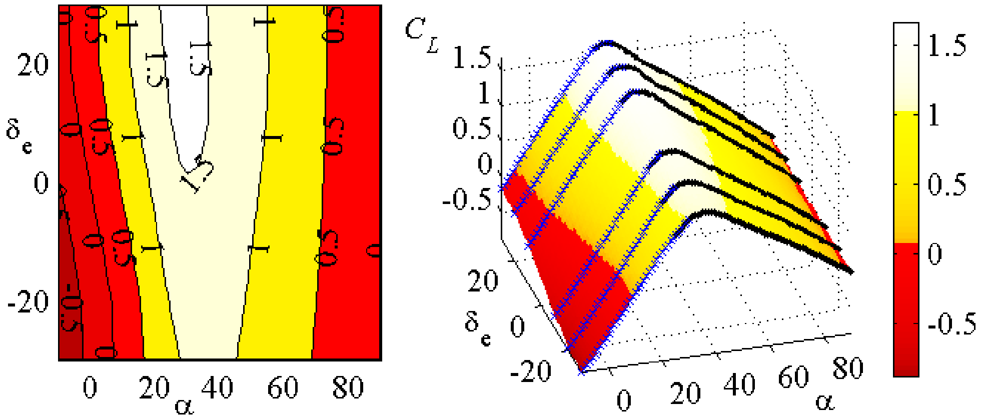

Figure 4.12: Contour (left) and 3D (right) plot of coefficient $C_L(\alpha, \bar{\delta}_e)$

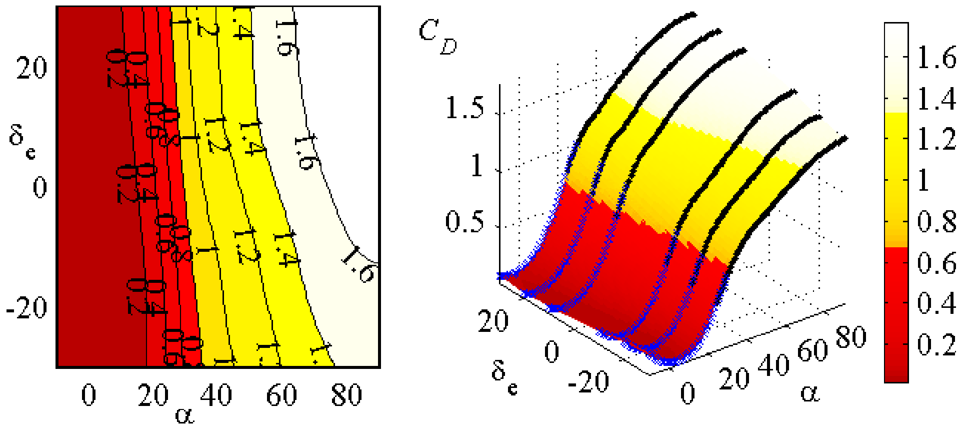

Figure 4.13: Contour (left) and 3D (right) plot of coefficient $C_D(\alpha, \bar{\delta}_e)$

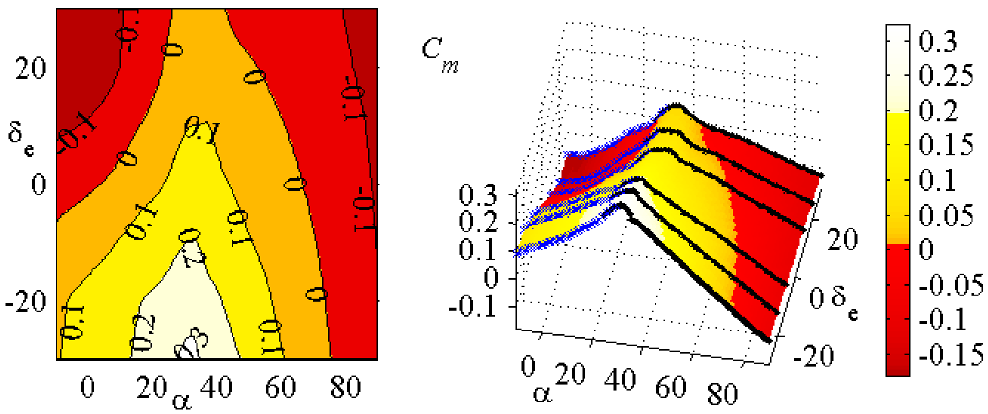

Figure 4.14: Contour (left) and 3D (right) plot of coefficient $C_m(\alpha, \bar{\delta}_e)$

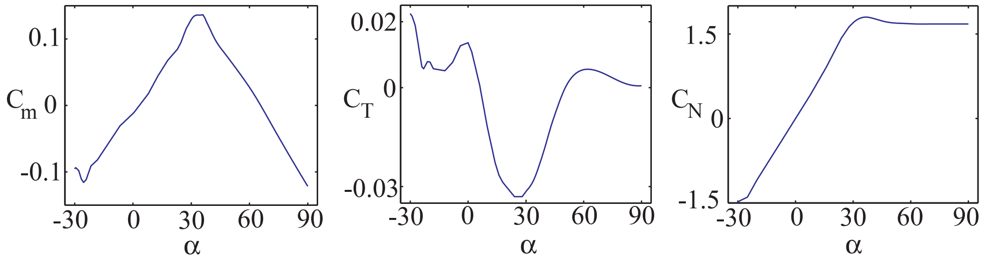

Figure 4.15: Output from virtual wind tunnel

4.4 Simulation

The new coefficient database has been tested in two ways. First of all, a sweep in angle of attack has been made with the help of "ADMIRE Extract & Plot" to determine whether the change from low to high angle of attack is smooth (see Figure 4.15. By changing a coefficient that does not depend on angle of attack, a step should be seen in the resulting plot. This has been done without remarks. Second, test flights where performed in FENIX. Besides looking for abrupt changes in performance, certain maneuvers were carried out.

A part of one test flight where a stall has been carried out can be seen in Figure 4.16. Slowly a pull up was performed with the help of a small positive stick input. When ADMIRE reached $\alpha \approx 35$ degrees, lift C_L and pitching moment C_m decrease radically and the Mach number becomes very low. The dimensionless pitching angular velocity $\bar{q}$ together with pitch attitude θ shows that the aircraft nose starts to descend. The control system tries to prevent this from happening by deflecting canard and elevon. When C_m reaches its lowest value maximum downward pitching acceleration $\dot{q}$ is reached. With the help of stick input, the angle of attack decreases and speed increases until a pull-up can be done.

No erratic behavior depending on aerodynamic data has been found during test flights. The sudden increase in pitching moment C_m can not be fully explained by canard and elevon deflection and is therefore assumed to depend on the original aerodynamics or on the combination of control system and aerodynamic data.

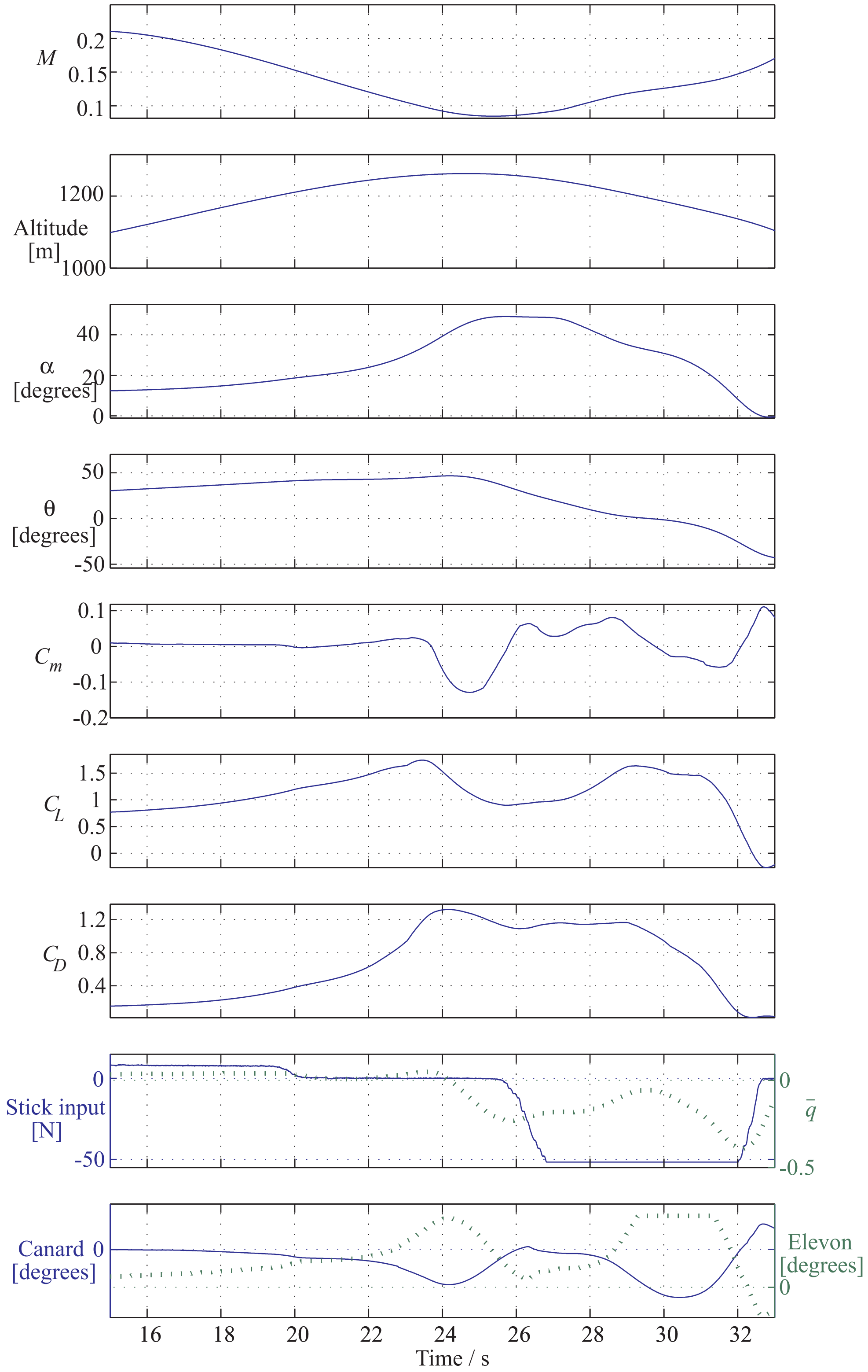

Figure 4.16: Output from FENIX. (The right labels belong to the dotted lines)

5. Conclusion

With the help of comparison with similar aircraft and gathered aerodynamic knowledge, a prediction of the ADMIRE's performance at high angle of attack has been performed.

The aircraft used for comparison has been the X-31A. This is simply because it resembles the ADMIRE and because the aerodynamic data has been available for high angles of attack. The comparison has not given as much help as expected because only the tendencies could be used. Also, the tangential force coefficient for the X-31A was hard to understand and the data for elevon was very sparse.

Tools to derive and visualize aerodynamic coefficients and for the development of new aerodynamic data have been developed. These tools are also partly prepared for the expanding of other coefficients than those expanded in this report.

The theory behind high angle of attack aerodynamics on canard delta aircraft has been explained and accounted for when the aerodynamics were derived. Together with the condition that the aircraft should have good properties without any erratic behavior, satisfactory aerodynamics for angles up to 90 degrees have been developed.

Transition from low angles of attack to high angles of attack has become very smooth. The old aerodynamics have not been tampered with which leaves the high angle of attack aerodynamic to be an add-on to the existing aerodynamics.

5.1 Assessment of Realism and Usefulness

During testing of the ADMIRE in FENIX, the aircraft has proved to have trustworthy properties and to be fully controllable with the current control system up to high angles of attack in the longitudinal direction. Stall has been performed and no deep stall tendencies have been found.

Since only longitudinal aerodynamics have been expanded in the angle of attack domain, the lateral motion is wrong above 30 degrees angle of attack. Especially roll angular acceleration $\dot{p}$ is too high since the elevon effectiveness should have decreased considerably after stall. This gives an unrealistically good controllability in the lateral direction. Prediction precision decreases with increasing angle of attack, still the important thing is that the aircraft has received the properties wanted.

For PIO research, the new angle of attack domain will be enough, while for research regarding spin ADMIRE most probably needs more aerodynamic data in lateral movement depending on both angle of attack and sideslip angle.

5.2 Further Work

With the material found and the tools made to expand the angle of attack for longitudinal coefficients, only theoretical problems remain before the angle of attack domain can be expanded for lateral coefficients. One of the theoretical problems is the asymmetric forces from vortices acting on the nose. One suggestion is to program random scale factors on the side force and roll moment coefficient to simulate this.

Another variable that could be extended is sideslip angle. Especially when spin is simulated, this variable range turns out to be far too small ($\pm 20^\circ$). Again, vortices around the nose will be hard to simulate and the coefficients hard to find.

Bibliography

[1] Hans Backström. Report on the usage of the Generic Aerodata Model. Technical report, SAAB Aircraft AB, SAAB Military Aircraft, S-58199 Linköping Sweden, may 1997. URL http://www.flyg.kth.se/misc-dir/DFM\&ADinfo.html. Download GAM at bottom of HTML page.

[2] Jenny Baer-Riedhart. F-18 HARV. Internet, Dec 2001. URL http://www.dfrc.nasa.gov/Projects/HARV/.

[3] Jenny Baer-Riedhart. X-31. Internet, Dec 2001. URL http://www.dfrc.nasa.gov/Projects/X31/home.html.

[4] Daniel W. Banks, Gregory M. Gatlin, and John W. Paulson Jr. Low-speed Longitudenal and Lateral-Directional Aerodynamic Characteristics of the X-31 Configuration. Technical Memorandum NASA TM-4351, National Aeronautics and Space Administration, Washington, DC 20546-0001, oct 1992. URL http://techreports.larc.nasa.gov/ltrs/PDF/tm4351.pdf. (No figures nor data in electronic document).

[5] A. Bergmann and D. Hummel. Aerodynamic Effects of Canard Position on a Wing Body Configuration in Symmetrical Flow. Technical Report AIAA-2001-0116, Institute of Fluid Mechanics, Technical University Braunschweig, Germany, Jan 2001.

[6] P. Champigny. High Angle of Attack Aerodynamics. AGARD Special Course, Office National d'Etudes et de Recherches Aérospatiales, 29, Avenue de la Division Leclerc, 92320 Chatillon, France. Presented at an AGARD Special Course on "Missile Aerodynamics", June 1994.

[7] L. Tu Eugene. Effect of Canard Deflection on Close-Coupled Canard-Wing-Body Aerodynamics. *Journal of Aircraft*, 31(1):138–145, Jan-Feb 1994. Presented as paper 92-2602 at the 10th AIAA Applied Aerodynamics Conference.

[8] Lars Forssell, Gunnar Hovmark, Åke Hyden, and Fredrik Johansson. The Aero-Data Model In a Research Environment ADMIRE for Flight Control Robustness Evaluation. Technical Report TP-119-7, GARTEUR FM(AG11), August 2001. Flight Clearance project.

[9] S.F. Hoerner. *Fluid-Dynamic Drag*. Published by author, 2 edition, 1958.

[10] D. Hummel and H.-Chr Oelker. Vortex Interference Effects on Close-Coupled Canard Configuration at Low Speed. Technical Report AGARD-CP-465, Institut für Strömnungsmechanik, Technische Universität Braunschweig, Germany, 1989.

[11] Fred Thomas Jane. *Jane's All the World's Aircraft 1986-87*. Jane's Yearbooks. Jane's Information Group, Coulsden, UK, 77th edition, 1986. ISBN 0 7106 1863.

[12] Fred Thomas Jane. *Jane's All the World's Aircraft 1996-97*. Jane's Yearbooks. Jane's Information Group, Coulsden, UK, 87th edition, 1996. ISBN 0 7106 1377 6.

[13] Leland Howard Jorgensen. Prediction of static aerodynamic characteristics for slender bodies alone and with lifting surfaces to very high angles of attack. Technical Report NASA TR R-474, Ames Research Center, Moffett Field, California, September 1977.

[14] *MATLAB Version 5.3*. The Mathworks, Inc., 2000. URL http://www.mathworks.com.

[15] Josef Rom. *High Angle of Attack Aerodynamics*. Springer-Verlag, New York, 1992. ISBN 0-387-97672-8.

[16] Tor Stavöstrand. Förekomst av Aerodynamiska Hysteres-Effekter. Technical report, SAAB, Gripen Systems and Flight Test, 1999. Report written for a course in Flight Mechanics at KTH.

[17] I.H. Tuncer, M.F. Platzer, and R.D. VanDyken. A Computional Study of a Close-Coupled Delta Canard-Wing-Body Configuration. AIAA 96-2440, Department of Aeronautics and Astronautics, Naval Postgraduate School, Monterey, California, 1996.

A. ADMIRE Coefficient Structure

The coefficient structure belonging to the generic model called GAM is as complex as the ones control system designers deal with in today's modern fighter aircraft. The datatable dimension belonging to each coefficient can be seen from the amount of input variables. The coefficients for Mach numbers above 0.4 have been excluded. Sideslip angle β, elevon asymmetry deflection angle and leading edge flap deflection angle are normalized with their maximum deflection angle (20°, 30° and 27°). *Sibeta*, *siday* and *sidai* mean that the sign of the variables *beta*, *day* and *dai* is used. The index "c" indicates that the input variable is normalized.

A.1 Longitudinal Coefficients for Mach Numbers Below 0.4

$$
\begin{aligned}
&C_{T_{basic}} = C_{T_{zero}}(M) + C_{T_h}(h,M)\\
&C_{T_{alpha}} = C_{T_{al}}(\alpha)\\
&C_{T_{dei}} = C_{T_{deal}}(\delta_{ei},\alpha)\cdot eieff\\
&C_{T_{dey}} = C_{T_{deal}}(\delta_{ey},\alpha)\cdot eoeff\\
&C_{T_{dedn}} = C_{T_{dnde}}(\delta_n,\delta_e,\alpha)\\
&C_{T_{dn}} = C_{T_{dnal}}(\delta_n,\alpha)\\
&C_{T_{dle}} = C_{T_{dleal}}(\delta_{le},\alpha) + C_{T_{lednal}}(\delta_n,\alpha)\cdot \tfrac{\delta_{le}}{27}\\
&C_{T_{beta}} = C_{T_{beta}}(\delta_n,\alpha)\cdot C_{T_{kb}}(|\beta|)\\
&C_{T_{da}} = C_{T_{daal}}(|\delta_{ai}|,|\alpha|)\cdot eieff + C_{T_{daal}}(|\delta_{ay}|,|\alpha|)\cdot eoeff\\
&C_{T_{dr}} = C_{T_{mdr}}(|\delta_r|,M)
\end{aligned}
\tag{A.1}
$$

$$
\begin{aligned}
\therefore C_T = \; & C_{T_{basic}} + C_{T_{alpha}} + C_{T_{dei}} + C_{T_{dey}} + C_{T_{dedn}} + C_{T_{dn}} + C_{T_{dle}} + C_{T_{beta}} +\\
& C_{T_{da}} + C_{T_{dr}}
\end{aligned}
$$

$$
\begin{aligned}
&C_{N_{basic}} = C_{N_{zero}}(M) + C_{N_{ezero}}(q_{a,corr},M)\\
&C_{N_{alfa}} = C_{N_{deal}}(0.0,\alpha)\cdot C_{N_{ea}}(q_{a,corr},M)\\
&C_{N_{dei}} = \left(C_{N_{deal}}(\delta_{ei},\alpha) - C_{N_{deal}}(0.0,\alpha)\right)\cdot eieff\cdot C_{N_{edei}}(q_{a,corr},M)\\
&C_{N_{dey}} = \left(C_{N_{deal}}(\delta_{ey},\alpha) - C_{N_{deal}}(0.0,\alpha)\right)\cdot eoeff\cdot C_{N_{edey}}(q_{a,corr},M)\\
&C_{N_{dedn}} = C_{N_{dnde}}(\delta_n,\delta_e,\alpha)\\
&C_{N_{dn}} = C_{N_{dnal}}(\delta_n,\alpha)\cdot C_{N_{edn}}(q_{a,corr},M)\\
&C_{N_{dle}} = \left(C_{N_{dleal}}(\alpha) + C_{N_{dldnal}}(\delta_n,\alpha) + C_{N_{dldeal}}(\delta_e,\alpha)\right)\cdot \tfrac{\delta_{le}}{27}\\
&C_{N_{cai}} = C_{N_{cai}}(cai,\alpha)\\
&C_{N_{beta}} = C_{N_{beta}}(\delta_n,\alpha)\cdot C_{N_{kb}}(|\beta|)\\
&C_{N_{alfad}} = C_{N_{adam}}(|\alpha|,M)\cdot\dot{\alpha}\\
&C_{N_q} = C_{N_{qal}}(|\alpha|)\cdot\hat{q}\cdot C_{N_{eq}}(q_{a,corr},M)\\
&C_{N_{nz}} = C_{N_{enz}}(q_{a,corr},M)\cdot(n_z-1)\\
&C_{N_{qd}} = C_{N_{eqd}}(q_{a,corr},M)\cdot\dot{q}
\end{aligned}
\tag{A.2}
$$

$$
\begin{aligned}
\therefore C_N = \; & C_{N_{basic}} + C_{N_{alfa}} + C_{N_{dei}} + C_{N_{dey}} + C_{N_{dedn}} + C_{N_{dn}} + C_{N_{dle}} + C_{N_{cai}} +\\
& C_{N_{beta}} + C_{N_{alfad}} + C_{N_q} + C_{N_{nz}} + C_{N_{qd}}
\end{aligned}
$$

$$
\begin{aligned}
&C_{m_{basic}} = C_{m_{zero}}(M) + C_{m_{ezero}}(q_{a,corr}, M)\\
&C_{m_{alfa}} = C_{m_{deal}}(0.0, \alpha) + C_{m_{ea}}(q_{a,corr}, M) \cdot \alpha\\
&C_{m_{dei}} = \left(C_{m_{deal}}(\delta_{ei}, \alpha) - C_{m_{deal}}(0.0, \alpha)\right) \cdot eieff \cdot C_{m_{edei}}(q_{a,corr}, M)\\
&C_{m_{dey}} = \left(C_{m_{deal}}(\delta_{ey}, \alpha) - C_{m_{deal}}(0.0, \alpha)\right) \cdot eoeff \cdot C_{m_{edey}}(q_{a,corr}, M)\\
&C_{m_{dedn}} = C_{m_{dnde}}(\delta_n, \delta_e, \alpha)\\
&C_{m_{dn}} = C_{m_{dnal}}(\delta_n, \alpha) \cdot C_{m_{edn}}(q_{a,corr}, M)\\
&C_{m_{dle}} = \left(C_{m_{dlal}}(\alpha) + C_{m_{dldea}}(\delta_e, \alpha) + C_{m_{dldna}}(\delta_n, \alpha)\right) \cdot \tfrac{\delta_{le}}{27} +\\
&\qquad\quad \left(C_{m_{edlei}}(q_{a,corr}, M) + C_{m_{edley}}(q_{a,corr}, M)\right) \cdot \tfrac{\delta_{le}}{27}\\
&C_{m_{cai}} = C_{m_{cai}}(cai, \alpha) + C_{m_{caidn}}(\delta_n, cai, \alpha)\\
&C_{m_{beta}} = C_{m_{beta}}(|\beta|, \delta_n, \alpha)\\
&C_{m_{da}} = C_{m_{daal}}(|\delta_{ai}|, \alpha) \cdot eieff + C_{m_{daal}}(|\delta_{ay}|, \alpha) \cdot eoeff\\
&C_{m_{alphad}} = C_{m_{adam}}(|\alpha|, M) \cdot \dot{\alpha}\\
&C_{m_q} = \left(C_{m_{qal}}(\alpha) + C_{m_{qdnal}}(\delta_n, \alpha)\right) \cdot \hat{q} \cdot C_{m_{eq}}(q_{a,corr}, M)\\
&C_{m_{nz}} = C_{m_{enz}}(q_{a,corr}, M) \cdot (n_z - 1)\\
&C_{m_{qd}} = C_{m_{eqd}}(q_{a,corr}, M) \cdot \dot{q}\\
&\therefore C_m = C_{m_{basic}} + C_{m_{alfa}} + C_{m_{dei}} + C_{m_{dey}} + C_{m_{dedn}} + C_{m_{dn}} + C_{m_{dle}} + C_{m_{cai}} +\\
&\qquad\quad C_{m_{beta}} + C_{m_{da}} + C_{m_{alphad}} + C_{m_q} + C_{m_{nz}} + C_{m_{qd}}
\end{aligned}
\tag{A.3}
$$

A.2 Lateral Coefficients for Mach Numbers Below 0.4

$$
\begin{aligned}
&C_{C_{beta}} = C_{C_{bal}}(|\beta|, \alpha) \cdot sibeta \cdot C_{C_{eb}}(q_{a,corr}, M)\\
&C_{C_{bde}} = \left(C_{C_{deb}}(|\beta|, \delta_{ei}, \alpha) \cdot eieff + C_{C_{deb}}(|\beta|, \delta_{ey}, \alpha) \cdot eoeff\right) \cdot sibeta\\
&C_{C_{bdn}} = C_{C_{dnb}}(|\beta|, \delta_n, \alpha) \cdot sibeta\\
&C_{C_{bdle}} = C_{C_{dleb}}(\delta_{le}, |\beta|, \alpha) \cdot sibeta\\
&C_{C_{bcai}} = C_{C_{bcai}}(cai, \alpha) \cdot \beta\\
&C_{C_{dr}} = C_{C_{bdral}}(|\beta|, \delta_r, \alpha) \cdot C_{C_{edr}}(q_{a,corr}, M)\\
&C_{C_{dai}} = \left(C_{C_{daal}}(|\delta_{ai}|, \alpha) \cdot sidai + \left(C_{C_{dal}}(\delta_{ei}, \alpha) - C_{C_{dal}}(0.0, \alpha)\right) \cdot \delta_{dai}\right) \cdot\\
&\qquad\quad eieff \cdot C_{C_{edai}}(q_{a,corr}, M)\\
&C_{C_{daib}} = C_{C_{dabal}}(|\alpha|) \cdot \left(|\delta_{ai}|/30.0\right) \cdot \left(|\beta|/20.0\right) \cdot eieff\\
&C_{C_{day}} = \left(C_{C_{daal}}(|\delta_{ay}|, \alpha) \cdot siday + \left(C_{C_{dal}}(\delta_{ey}, \alpha) - C_{C_{dal}}(0.0, \alpha)\right) \cdot \delta_{day}\right) \cdot\\
&\qquad\quad eoeff + C_{C_{eday}}(q_{a,corr}, M) \cdot \delta_{day}\\
&C_{C_{dayb}} = C_{C_{dabal}}(|\alpha|) \cdot \left(|\delta_{ay}|/30.0\right) \cdot \left(|\beta|/20.0\right) \cdot eoeff\\
&C_{C_{dna}} = C_{C_{dnaal}}(\delta_{ne}, \alpha) \cdot \delta_{na}\\
&C_{C_{betad}} = C_{C_{bdl}}(\alpha) \cdot \dot{\beta}\\
&C_{C_p} = C_{C_{pal}}(\alpha) \cdot p_c\\
&C_{C_{pbeta}} = C_{C_{pba}}(|\beta|, \alpha) \cdot p_c\\
&C_{C_r} = C_{C_{ral}}(\delta_n, \alpha) \cdot r_c\\
&C_{C_{rbeta}} = C_{C_{rba}}(|\beta|, |\alpha|) \cdot r_c\\
&\therefore C_C = C_{C_{beta}} + C_{C_{bde}} + C_{C_{bdn}} + C_{C_{bdle}} + C_{C_{bcai}} + C_{C_{dr}} + C_{C_{dai}} + C_{C_{daib}} +\\
&\qquad\quad C_{C_{day}} + C_{C_{dayb}} + C_{C_{dna}} + C_{C_{betad}} + C_{C_p} + C_{C_{pbeta}} + C_{C_r} + C_{C_{rbeta}}
\end{aligned}
\tag{A.4}
$$

$$
\begin{aligned}
&C_{n_{basic}} = C_{n_{zero}}\left(|\alpha|\right)\\
&C_{n_{beta}} = C_{n_{bal}}\left(|\beta|,\alpha\right)\cdot sibeta + C_{n_{eb}}\left(q_{a,corr},M\right)\cdot\beta\\
&C_{n_{bde}} = \left(C_{n_{deb}}\left(|\beta|,\delta_{ei},\alpha\right)\cdot eieff + C_{n_{deb}}\left(|\beta|,\delta_{ey},\alpha\right)\cdot eoeff\right)\cdot sibeta\\
&C_{n_{bdn}} = C_{n_{dnb}}\left(|\beta|,\delta_{n},\alpha\right)\cdot sibeta\\
&C_{n_{bdle}} = \left(C_{n_{dleb}}\left(\delta_{le},|\beta|,\delta_{ei},\alpha\right)\cdot eieff + C_{n_{dleb}}\left(\delta_{le},|\beta|,\delta_{ey},\alpha\right)\cdot eoeff\right)\cdot sibeta\\
&C_{n_{cai}} = C_{n_{bcai}}\left(cai,\alpha\right)\cdot\beta\\
&C_{n_{dr}} = C_{n_{bdral}}\left(\beta,\delta_{r},\alpha\right)\cdot C_{n_{edr}}\left(q_{a,corr},M\right)\\
&C_{n_{dai}} = \left(C_{n_{daal}}\left(|\delta_{ai}|,\alpha\right)\cdot sidai + \left(C_{n_{dal}}\left(\delta_{ei},\alpha\right) - C_{n_{dal}}\left(0.0,\alpha\right)\right)\cdot\delta_{ai}\right)\cdot\\
&\qquad eieff\cdot C_{n_{edai}}\left(q_{a,corr},M\right)\\
&C_{n_{daib}} = C_{n_{dabal}}\left(|\alpha|\right)\cdot\left(\frac{|\delta_{ai}|}{30.0}\right)\cdot\left(\frac{|\beta|}{20.0}\right)\cdot eieff\\
&C_{n_{day}} = \left(C_{n_{daal}}\left(|\delta_{ay}|,\alpha\right)\cdot siday + \left(C_{n_{dal}}\left(\delta_{ey},\alpha\right) - C_{n_{dal}}\left(0.0,\alpha\right)\right)\cdot\delta_{ay}\right)\cdot\\
&\qquad eoeff + C_{n_{eday}}\left(q_{a,corr},M\right)\cdot\delta_{ay}\\
&C_{n_{dayb}} = C_{n_{dabal}}\left(|\alpha|\right)\cdot\left(|\delta_{ay}|/30.0\right)\cdot\left(|\beta|/20.0\right)\cdot eoeff\\
&C_{n_{dna}} = C_{n_{dnaal}}\left(\delta_{ne},\alpha\right)\cdot\delta_{na}\\
&C_{n_{betad}} = C_{n_{bdl}}\left(\alpha\right)\cdot\dot{\beta}\\
&C_{n_{p}} = \left(C_{n_{pal}}\left(\delta_{n},\alpha\right) + C_{n_{ep}}\left(q_{a,corr},M\right)\right)\cdot p_{c}\\
&C_{n_{pbeta}} = C_{n_{pba}}\left(|\beta|,\alpha\right)\cdot p_{c}\\
&C_{n_{r}} = C_{n_{ral}}\left(\delta_{n},\alpha\right)\cdot r_{c}\cdot C_{n_{er}}\left(q_{a,corr},M\right)\\
&C_{n_{rbeta}} = C_{n_{rba}}\left(|\beta|,\alpha\right)\cdot r_{c}
\end{aligned}
\tag{A.5}
$$

$$
\begin{aligned}
\therefore C_n = \; & C_{n_{basic}} + C_{n_{beta}} + C_{n_{bde}} + C_{n_{bdn}} + C_{n_{bdle}} + C_{n_{cai}} + C_{n_{dr}} + C_{n_{dai}} +\\
& C_{n_{daib}} + C_{n_{day}} + C_{n_{dayb}} + C_{n_{dna}} + C_{n_{betad}} + C_{n_{p}} + C_{n_{pbeta}} + C_{n_{r}} + C_{n_{rbeta}}
\end{aligned}
$$

$$
\begin{aligned}
&C_{l_{basic}} = C_{l_{zero}}\left(|\alpha|\right)\\
&C_{l_{beta}} = C_{l_{bal}}\left(|\beta|,\alpha\right)\cdot sibeta + C_{l_{eb}}\left(q_{a,corr},M\right)\cdot\beta\\
&C_{l_{bde}} = \left(C_{l_{deb}}\left(|\beta|,\delta_{ei},\delta_{n},\alpha\right)\cdot eieff + C_{l_{deb}}\left(|\beta|,\delta_{ey},\delta_{n},\alpha\right)\cdot eoeff\right)\cdot sibeta\\
&C_{l_{bdn}} = C_{l_{dnb}}\left(|\beta|,\delta_{n},\alpha\right)\cdot sibeta\\
&C_{l_{bdle}} = \left(C_{l_{dleb}}\left(\delta_{le},|\beta|,\delta_{ei},\alpha\right)\cdot eieff + C_{l_{dleb}}\left(\delta_{le},|\beta|,\delta_{ey},\alpha\right)\cdot eoeff\right)\cdot sibeta\\
&C_{\delta l_{r}} = C_{l_{bdral}}\left(|\beta|,\delta_{r},\alpha\right)\cdot C_{l_{edr}}\left(q_{a,corr},M\right)\\
&C_{l_{dai}} = \left(C_{l_{daal}}\left(|\delta_{ai}|,\alpha\right)\cdot sidai + \left(C_{l_{dal}}\left(\delta_{ei},\alpha\right) - C_{l_{dal}}\left(0,\alpha\right)\right)\cdot\delta_{ai}\right)\cdot eieff\cdot\\
&\qquad C_{l_{edai}}\left(q_{a,corr},M\right)\\
&C_{l_{daib}} = C_{l_{dabal}}\left(|\alpha|\right)\cdot\left(\frac{|\delta_{ai}|}{30.0}\right)\cdot\left(\frac{|\beta|}{20.0}\right)\cdot eieff\\
&C_{l_{day}} = \left(C_{l_{daal}}\left(|\delta_{ay}|,\alpha\right)\cdot siday + \left(C_{l_{dal}}\left(\delta_{ey},\alpha\right) - C_{l_{dal}}\left(0,\alpha\right)\right)\cdot\delta_{ay}\right)\cdot eoeff\cdot\\
&\qquad C_{l_{eday}}\left(q_{a,corr},M\right)\\
&C_{l_{dayb}} = C_{l_{dabal}}\left(|\alpha|\right)\cdot\left(\frac{|\delta_{ay}|}{30.0}\right)\cdot\left(\frac{|\beta|}{20.0}\right)\cdot eoeff\\
&C_{l_{dna}} = C_{l_{dnaal}}\left(\delta_{ne},\alpha\right)\cdot\delta_{na}\\
&C_{l_{betad}} = C_{l_{bdl}}\left(\alpha\right)\cdot\dot{\beta}\\
&C_{l_{p}} = C_{l_{pal}}\left(\delta_{n},\alpha\right)\cdot p_{c}\cdot C_{n_{ep}}\left(q_{a,corr},M\right)\\
&C_{n_{pbeta}} = C_{l_{pba}}\left(|\beta|,\alpha\right)\cdot p_{c}\\
&C_{l_{r}} = C_{l_{ral}}\left(\delta_{n},\alpha\right)\cdot r_{c}\\
&C_{l_{rbeta}} = C_{l_{rba}}\left(|\beta|,\alpha\right)\cdot r_{c}\\
&C_{l_{rde}} = C_{l_{rdem}}\left(M\right)\cdot C_{l_{rka}}\left(|\alpha|\right)\cdot\left(eieff\cdot\frac{\delta_{ei}}{30.0} + eoeff\cdot\frac{\delta_{ey}}{30.0}\right)\cdot r_{c}
\end{aligned}
\tag{A.6}
$$

$$
\begin{aligned}
\therefore C_l = \; & C_{l_{basic}} + C_{l_{beta}} + C_{l_{bde}} + C_{l_{bdn}} + C_{l_{bdle}} + C_{\delta l_{r}} + C_{l_{dai}} + C_{l_{daib}} +\\
& C_{l_{day}} + C_{l_{dayb}} + C_{l_{dna}} + C_{l_{betad}} + C_{l_{p}} + C_{n_{pbeta}} + C_{l_{r}} + C_{l_{rbeta}} + C_{l_{rde}}
\end{aligned}
$$

A.3 Original GAM coefficients

This is extracted from GAM's .aer files to show how the longitudinal coefficients are named internally. The explanation is SAAB's own as well as the use of abbreviations, see [1] for further explanation.

Coefficient			Variable required		
in GAM domain	Explanation	Speed domain	First	Second	Third
CNADAM	Alpha-dot deriv	high speed.	ALFA	M	
CNBETA	Incr. due to side slip.		DN	ALFA	
CNCAI	Incr.due to engine mass flow ratio.		CAI	ALFA	
CNDEAL	Elevator efficiency	low speed.	DE	ALFA	
CNDEYODE	Outboard elevon efficiency.		ALFA	M	
CNDLDEAL	L-E flap eff. de-depend	low speed.	DE	ALFA	
CNDLDNAL	L-E flap eff. dn-depend	low speed.	DN	ALFA	
CNDLEAL	L-E flap efficiency	low speed.	ALFA		
CNDNAL	Canard efficiency	low speed.	DN	ALFA	
CNDNDE	Incr. at combined de-dn.		DN	DE	ALFA
CNDNH	Canard efficiency	high speed.	ALFA	DN	M
CNEA	Elast. on alfa-dependency.		QA	M	
CNEDEI	Elast. on dei-efficiency.		QA	M	
CNEDEY	Elast. on dey-efficiency.		QA	M	
CNEDN	Elast. on dn-efficiency.		QA	M	
CNENZ	Elast incr.due to nz.		QA	M	
CNEQ	Elast. due to q.		QA	M	
CNEQD	Elast incr.due to q-dot.		QA	M	
CNEZERO	Elast.incr. to zero value.		QA	M	
CNKB	Interpol.function, side slip.		BETA		
CNLBRDEA	Incr due to air brake	low speed.	DE	ALFA	
CNLBRM	Incr due to air brake	high speed.	DLBR	M	
CNLST	Incr. due to landing gear.		BETA	ALFA	
CNMDEA	Elevator efficiency	high speed.	M	DE	ALFA
CNMDLEA	L-E flap efficiency	high speed.	M	DLE	ALFA
CNQAL	Q-derivative	low speed.	ALFA		
CNQAM	Q-derivative	high speed.	ALFA	M	
CNZERO	Zero value.		M		
CPMADAM	Derivative wrt alfa-dot.		ALFA	M	
CPMBETA	Incr. due to side slip.		BETA	DN	ALFA
CPMCAI	Incr. due to engine mass flow rate.		CAI	ALFA	
CPMCAIDN	Incr. in CAI-efficiency due to dn.		DN	CAI	ALFA
CPMDAAL	Incr. due to aileron	low speed.	DA	ALFA	
CPMDEAL	Elevator efficiency	low speed.	DE	ALFA	
CPMDEYOD	Outboard elevon efficiency.		ALFA	M	
CPMDLAL	L-E flap efficiency	low speed.	ALFA		
CPMDLDEA	L-E flap eff. de-dependency	low speed.	DE	ALFA	
CPMDLDNA	L-E flap eff. de-dependency	low speed.	DN	ALFA	
CPMDNAL	Canard efficiency	low speed.	DN	ALFA	
CPMDNDE	Incr. at combined de-dn.		DN	DE	ALFA
CPMEA	Elast. on alfa-dependency.		QA	M	
CPMEDEI	Elast. on dei-efficiency.		QA	M	
CPMEDEY	Elast. on dey-efficiency.		QA	M	
CPMEDLEI	Elast. on dlei-efficiency.		QA	M	
CPMEDLEY	Elast. on dley-efficiency.		QA	M	
CPMEDN	Elast. on dn-efficiency.		QA	M	
CPMENZ	Elast incr. due to nz.		QA	M	
CPMEQ	Elast. due to q.		QA	M	
CPMEQD	Elast incr. due to q-dot.		QA	M	
CPMEZERO	Elast. incr. to zero value.		QA	M	
CPMLBRDA	Incr. due to air brake	low speed.	DE	ALFA	
CPMLBRM	Incr. due to air brake	high speed.	DLBR	M	
CPMLST	Incr. due to landing gear.		BETA	ALFA	
CPMMDEA	Elevator efficiency	high speed.	M	DE	ALFA
CPMMDLEA	L-E flap efficiency	high speed.	M	DLE	ALFA
CPMMDNA	Canard efficiency	high speed.	M	DN	ALFA
CPMQAL	Q-derivative	low speed.	ALFA		
CPMQAM	Q-derivative	high speed.	ALFA	M	
CPMQDNAL	Q-deriv. dn-dependency low speed.		DN	ALFA	
CPMZERO	Zero value.		M		
CTAL	Alpha dependency	low speed.	ALFA		
CTBETA	Incr. due to side slip.		DN	ALFA	
CTDAAL	Incr. due to aileron	low speed.	DA	ALFA	
CTDAM	Incr. due to aileron	high speed.	DA	M	
CTDEAL	Elevator efficiency	low speed.	DE	ALFA	
CTDEYODE	Outboard elevon efficiency.		M		
CTDLEAL	L-E flap efficiency	low speed.	DLE	ALFA	
CTDNAL	Canard efficiency	low speed.	DN	ALFA	
CTDNDE	Incr. at combined de-dn.		DN	DE	ALFA
CTH	Zero value & altitude dependency.		H	M	
CTKB	Interpolation function.		BETA		
CTLBRDEA	Incr. due to air brake	low speed.	DE	ALFA	
CTLBRM	Incr. due to air brake	high speed.	DLBR	M	
CTLEDNAL	L-E flap efficiency dn=-40gr	low speed.	DN	ALFA	
CTLST	Incr. due to landing gear.		BETA	ALFA	
CTMA	Incr. due to alpha	high speed.	M	ALFA	
CTMDEA	Elevator efficiency	high speed.	M	DE	ALFA
CTMDLEA	L-E flap efficiency	high speed.	M	DLE	ALFA
CTMDNA	Canard efficiency	high speed.	M	DN	ALFA
CTMDR	Rudder efficiency.		DR	M	
CTZERO	Zero value.		M		

B. ADMIRE High Angle of Attack in AER format

B.1 Basic increments for $C_m(\alpha)$, $C_N(\alpha)$ and $C_T(\alpha)$

CPMHZERO
Basic Cm increment at high aoa, low speed.
020110
1
ALFA

-10	0
30	0
31	0.00393702
32	0.00611439
33	0.00696266
34	0.00680104
35	0.0068876
36	0.00745795
37	0.00288654
38	-0.00403471
39	-0.00979179
40	-0.0160015
41	-0.0223403
42	-0.0281654
43	-0.0332625
44	-0.0377787
45	-0.0418731
46	-0.0457044
47	-0.0494315
48	-0.0531876
49	-0.0569955
50	-0.0608478
51	-0.0647369
52	-0.0686556
53	-0.0725964
54	-0.0765535
55	-0.0805343
56	-0.0845522
57	-0.0886211
58	-0.0927544
59	-0.0969658
60	-0.101269
61	-0.105677
62	-0.110205
63	-0.114863
64	-0.119646
65	-0.124535
66	-0.129513
67	-0.134564
68	-0.139669
69	-0.14481
70	-0.149971
71	-0.155134
72	-0.160282
73	-0.165409
74	-0.170514
75	-0.175599
76	-0.180662
77	-0.185705
78	-0.190727
79	-0.19573
80	-0.200713
81	-0.205676
82	-0.21062
83	-0.215545
84	-0.220452
85	-0.22534
86	-0.23021
87	-0.235062
88	-0.239896
89	-0.244713
90	-0.249514

CNHZERO
Basic CN increment at high aoa, low speed.
020110
1
ALFA

-10	0
30	0
31	0.0294658
32	0.0528843
33	0.0711848
34	0.0852009
35	0.0950007
36	0.100283
37	0.100811
38	0.0971894
39	0.0906064
40	0.0822615
41	0.0731041
42	0.0634197
43	0.053387
44	0.0432897
45	0.0335581
46	0.0246333
47	0.0169252
48	0.0105042
49	0.00523344
50	0.000972991
51	-0.0024171
52	-0.00507687
53	-0.00715279
54	-0.00880106
55	-0.0101787
56	-0.0114428
57	-0.0127503
58	-0.0142345
59	-0.0158591
60	-0.0175141
61	-0.0190892
62	-0.0204741
63	-0.0215586
64	-0.0222453
65	-0.0225592
66	-0.0225917
67	-0.0224352
68	-0.022182
69	-0.0219242
70	-0.0217535
71	-0.0217114
72	-0.0217479
73	-0.0218041
74	-0.0218436
75	-0.0218658
76	-0.021873
77	-0.0218678
78	-0.0218527
79	-0.0218301
80	-0.0218025
81	-0.0217723
82	-0.0217421
83	-0.0217143
84	-0.0216914
85	-0.0216758
86	-0.0216701
87	-0.0216767
88	-0.021698
89	-0.0217365
90	-0.0217948

CTHZERO
Basic CT increment at high aoa, low speed.
020110
1
ALFA

-10	0
30	0
31	0.000712537
32	0.00144353
33	0.00230658
34	0.00341404
35	0.00480371
36	0.00639883
37	0.00811293
38	0.00988454
39	0.0117243
40	0.0136556
41	0.0156875
42	0.0177463
43	0.0197293
44	0.0215695
45	0.0232992
46	0.0249683
47	0.0266056
48	0.0281814
49	0.0296562
50	0.0309904
51	0.0321593
52	0.0331708
53	0.0340368
54	0.0347695
55	0.0353808
56	0.0358829
57	0.0362875
58	0.0366031
59	0.0368371
60	0.0369964
61	0.0370882
62	0.0371197
63	0.0370979
64	0.0370299
65	0.0369222
66	0.0367787
67	0.0366032
68	0.0363996
69	0.0361716
70	0.035923
71	0.0356576
72	0.0353791
73	0.0350913
74	0.0347981
75	0.0345031
76	0.0342102
77	0.0339231
78	0.0336455
79	0.0333813
80	0.0331342
81	0.0329079
82	0.0327062
83	0.0325309
84	0.0323831
85	0.0322637
86	0.0321736
87	0.0321137
88	0.0320849
89	0.0320882
90	0.0321244

B.2 $C_m(\bar{\delta}_n, \alpha)$

CPMHDN
Increment due to canard at high aoa, low speed.
020119
2
DN
ALFA

-55	-10	0
-55	30	0
-55	31	-0.194961
-55	32	-0.196650
-55	33	-0.197407
-55	34	-0.197283
-55	35	-0.197415
-55	36	-0.198111
-55	37	-0.193828
-55	38	-0.187444
-55	39	-0.182556
-55	40	-0.177609
-55	41	-0.172890
-55	42	-0.168975
-55	43	-0.166014
-55	44	-0.163793
-55	45	-0.162087
-55	46	-0.160675
-55	47	-0.159391
-55	48	-0.158135
-55	49	-0.156917
-55	50	-0.155779
-55	51	-0.154763
-55	52	-0.153910
-55	53	-0.153257
-55	54	-0.152796
-55	55	-0.152474
-55	56	-0.152230
-55	57	-0.152006
-55	58	-0.151741
-55	59	-0.151376
-55	60	-0.150852
-55	61	-0.150130
-55	62	-0.149201
-55	63	-0.148060
-55	64	-0.146718
-55	65	-0.145198
-55	66	-0.143525
-55	67	-0.141722
-55	68	-0.139815
-55	69	-0.137835
-55	70	-0.135813
-55	71	-0.133781
-55	72	-0.131769
-55	73	-0.129797
-55	74	-0.127880
-55	75	-0.126029
-55	76	-0.124245
-55	77	-0.122529
-55	78	-0.120877
-55	79	-0.119287
-55	80	-0.117759
-55	81	-0.116290
-55	82	-0.114879
-55	83	-0.113523
-55	84	-0.112222
-55	85	-0.110973
-55	86	-0.109775
-55	87	-0.108626
-55	88	-0.107524
-55	89	-0.106467
-55	90	-0.105454
-45	-10	0
-45	30	0
-45	31	-0.169959
-45	32	-0.170480
-45	33	-0.169631
-45	34	-0.167750
-45	35	-0.166282
-45	36	-0.165648
-45	37	-0.160334
-45	38	-0.153105
-45	39	-0.147437
-45	40	-0.141674
-45	41	-0.136101
-45	42	-0.131321
-45	43	-0.127522
-45	44	-0.124551
-45	45	-0.122242
-45	46	-0.120434
-45	47	-0.118960
-45	48	-0.117683
-45	49	-0.116566
-45	50	-0.115596
-45	51	-0.114758
-45	52	-0.114039
-45	53	-0.113424
-45	54	-0.112897
-45	55	-0.112428
-45	56	-0.111979
-45	57	-0.111512
-45	58	-0.110988
-45	59	-0.110369
-45	60	-0.109618
-45	61	-0.108698
-45	62	-0.107593
-45	63	-0.106304
-45	64	-0.104855
-45	65	-0.103277
-45	66	-0.101603
-45	67	-0.099864
-45	68	-0.098094
-45	69	-0.096325
-45	70	-0.094589
-45	71	-0.092916
-45	72	-0.091327
-45	73	-0.089831
-45	74	-0.088431
-45	75	-0.087127
-45	76	-0.085922
-45	77	-0.084817
-45	78	-0.083815
-45	79	-0.082917
-45	80	-0.082124
-45	81	-0.081437
-45	82	-0.080846
-45	83	-0.080340
-45	84	-0.079910
-45	85	-0.079545
-45	86	-0.079235
-45	87	-0.078970
-45	88	-0.078740
-45	89	-0.078534
-45	90	-0.078342
-35	-10	0
-35	30	0
-35	31	-0.148496
-35	32	-0.148930
-35	33	-0.148510
-35	34	-0.147465
-35	35	-0.146996
-35	36	-0.147312
-35	37	-0.142760
-35	38	-0.136105
-35	39	-0.130834
-35	40	-0.125303
-35	41	-0.119809
-35	42	-0.114970
-35	43	-0.111002
-35	44	-0.107771
-35	45	-0.105132
-35	46	-0.102942
-35	47	-0.101054
-35	48	-0.099351
-35	49	-0.097823
-35	50	-0.096493
-35	51	-0.095365
-35	52	-0.094419
-35	53	-0.093629
-35	54	-0.092969
-35	55	-0.092399
-35	56	-0.091874
-35	57	-0.091346
-35	58	-0.090771
-35	59	-0.090102
-35	60	-0.089293
-35	61	-0.088303
-35	62	-0.087120
-35	63	-0.085749
-35	64	-0.084214
-35	65	-0.082549
-35	66	-0.080788
-35	67	-0.078966
-35	68	-0.077117
-35	69	-0.075275
-35	70	-0.073475
-35	71	-0.071749
-35	72	-0.070115
-35	73	-0.068573
-35	74	-0.067119
-35	75	-0.065745
-35	76	-0.064447
-35	77	-0.063219
-35	78	-0.062054
-35	79	-0.060947
-35	80	-0.059892
-35	81	-0.058883
-35	82	-0.057915
-35	83	-0.056981
-35	84	-0.056076
-35	85	-0.055194
-35	86	-0.054329
-35	87	-0.053476
-35	88	-0.052627
-35	89	-0.051779
-35	90	-0.050924
-25	-10	0
-25	30	0
-25	31	-0.128547
-25	32	-0.129201
-25	33	-0.129546
-25	34	-0.129043
-25	35	-0.128813
-25	36	-0.129128
-25	37	-0.124402
-25	38	-0.117465
-25	39	-0.111869
-25	40	-0.106037
-25	41	-0.100319
-25	42	-0.095352
-25	43	-0.091344
-25	44	-0.088137
-25	45	-0.085564
-25	46	-0.083457
-25	47	-0.081649
-25	48	-0.079998
-25	49	-0.078471
-25	50	-0.077065
-25	51	-0.075768
-25	52	-0.074573
-25	53	-0.073468
-25	54	-0.072443
-25	55	-0.071474
-25	56	-0.070529
-25	57	-0.069579
-25	58	-0.068594
-25	59	-0.067553
-25	60	-0.066444
-25	61	-0.065251
-25	62	-0.063961
-25	63	-0.062562
-25	64	-0.061061
-25	65	-0.059473
-25	66	-0.057817
-25	67	-0.056109
-25	68	-0.054367
-25	69	-0.052610
-25	70	-0.050856

-25	71	-0.049126
-25	72	-0.047440
-25	73	-0.045805
-25	74	-0.044224
-25	75	-0.042699
-25	76	-0.041233
-25	77	-0.039826
-25	78	-0.038482
-25	79	-0.037202
-25	80	-0.035988
-25	81	-0.034843
-25	82	-0.033767
-25	83	-0.032764
-25	84	-0.031835
-25	85	-0.030983
-25	86	-0.030209
-25	87	-0.029515
-25	88	-0.028904
-25	89	-0.028377
-25	90	-0.027937
-15	-10	0
-15	30	0
-15	31	-0.102553
-15	32	-0.101882
-15	33	-0.100222
-15	34	-0.098335
-15	35	-0.097463
-15	36	-0.097744
-15	37	-0.093456
-15	38	-0.087290
-15	39	-0.082665
-15	40	-0.077883
-15	41	-0.073234
-15	42	-0.069334
-15	43	-0.066370
-15	44	-0.064167
-15	45	-0.062540
-15	46	-0.061303
-15	47	-0.060270
-15	48	-0.059301
-15	49	-0.058379
-15	50	-0.057524
-15	51	-0.056750
-15	52	-0.056076
-15	53	-0.055518
-15	54	-0.055091
-15	55	-0.054793
-15	56	-0.054589
-15	57	-0.054441
-15	58	-0.054306
-15	59	-0.054144
-15	60	-0.053915
-15	61	-0.053577
-15	62	-0.053091
-15	63	-0.052435
-15	64	-0.051616
-15	65	-0.050653
-15	66	-0.049565
-15	67	-0.048372
-15	68	-0.047093
-15	69	-0.045747
-15	70	-0.044352
-15	71	-0.042931
-15	72	-0.041505
-15	73	-0.040087
-15	74	-0.038684
-15	75	-0.037300
-15	76	-0.035943
-15	77	-0.034617
-15	78	-0.033329
-15	79	-0.032085
-15	80	-0.030890
-15	81	-0.029751
-15	82	-0.028672
-15	83	-0.027660
-15	84	-0.026722
-15	85	-0.025861
-15	86	-0.025086
-15	87	-0.024401
-15	88	-0.023812
-15	89	-0.023325
-15	90	-0.022946
-5	-10	0
-5	30	0
-5	31	-0.037023
-5	32	-0.037862
-5	33	-0.036366
-5	34	-0.034032
-5	35	-0.034421
-5	36	-0.039759
-5	37	-0.042991
-5	38	-0.043589
-5	39	-0.043974
-5	40	-0.042869
-5	41	-0.040964
-5	42	-0.039264
-5	43	-0.038257
-5	44	-0.037818
-5	45	-0.037772
-5	46	-0.037942
-5	47	-0.038151
-5	48	-0.038249
-5	49	-0.038198
-5	50	-0.038015
-5	51	-0.037727
-5	52	-0.037360
-5	53	-0.036943
-5	54	-0.036502
-5	55	-0.036047
-5	56	-0.035587
-5	57	-0.035127
-5	58	-0.034672
-5	59	-0.034228
-5	60	-0.033779
-5	61	-0.033300
-5	62	-0.032769
-5	63	-0.032163
-5	64	-0.031479
-5	65	-0.030724
-5	66	-0.029906
-5	67	-0.029033
-5	68	-0.028111
-5	69	-0.027148
-5	70	-0.026152
-5	71	-0.025142
-5	72	-0.024138
-5	73	-0.023150
-5	74	-0.022182
-5	75	-0.021239
-5	76	-0.020323
-5	77	-0.019439
-5	78	-0.018589
-5	79	-0.017778
-5	80	-0.017010
-5	81	-0.016287
-5	82	-0.015614
-5	83	-0.014995
-5	84	-0.014432
-5	85	-0.013930
-5	86	-0.013492
-5	87	-0.013122
-5	88	-0.012824
-5	89	-0.012600
-5	90	-0.012456
0	-10	0
0	30	0
0	31	0
0	32	0
0	33	0
0	34	0
0	35	0
0	36	0
0	37	0
0	38	0
0	39	0
0	40	0
0	41	0
0	42	0
0	43	0
0	44	0
0	45	0
0	46	0
0	47	0
0	48	0
0	49	0
0	50	0
0	51	0
0	52	0
0	53	0
0	54	0
0	55	0
0	56	0
0	57	0
0	58	0
0	59	0
0	60	0
0	61	0
0	62	0
0	63	0
0	64	0
0	65	0
0	66	0
0	67	0
0	68	0
0	69	0
0	70	0
0	71	0
0	72	0
0	73	0
0	74	0
0	75	0
0	76	0
0	77	0
0	78	0
0	79	0
0	80	0
0	81	0
0	82	0
0	83	0
0	84	0
0	85	0
0	86	0
0	87	0
0	88	0
0	89	0
0	90	0
5	-10	0
5	30	0
5	31	0.023449
5	32	0.021456
5	33	0.019668
5	34	0.018114
5	35	0.015461
5	36	0.011384
5	37	0.011412
5	38	0.012650
5	39	0.011483
5	40	0.009519
5	41	0.007018
5	42	0.004145
5	43	0.001402
5	44	-0.000956
5	45	-0.002908
5	46	-0.004438
5	47	-0.005526
5	48	-0.006177
5	49	-0.006470
5	50	-0.006492
5	51	-0.006331
5	52	-0.006075
5	53	-0.005810
5	54	-0.005621
5	55	-0.005542
5	56	-0.005559
5	57	-0.005653
5	58	-0.005806
5	59	-0.006002
5	60	-0.006221
5	61	-0.006446
5	62	-0.006658
5	63	-0.006829
5	64	-0.006948
5	65	-0.007012

5	66	-0.007020
5	67	-0.006971
5	68	-0.006863
5	69	-0.006695
5	70	-0.006465
5	71	-0.006174
5	72	-0.005839
5	73	-0.005475
5	74	-0.005093
5	75	-0.004703
5	76	-0.004314
5	77	-0.003936
5	78	-0.003580
5	79	-0.003254
5	80	-0.002969
5	81	-0.002734
5	82	-0.002559
5	83	-0.002454
5	84	-0.002429
5	85	-0.002493
5	86	-0.002657
5	87	-0.002929
5	88	-0.003321
5	89	-0.003841
5	90	-0.004499
15	-10	0
15	30	0
15	31	0.010509
15	32	0.006093
15	33	0.002565
15	34	-0.000432
15	35	-0.004327
15	36	-0.009505
15	37	-0.010276
15	38	-0.009234
15	39	-0.009693
15	40	-0.009838
15	41	-0.009837
15	42	-0.010207
15	43	-0.011044
15	44	-0.012085
15	45	-0.013153
15	46	-0.014141
15	47	-0.014945
15	48	-0.015484
15	49	-0.015789
15	50	-0.015920
15	51	-0.015919
15	52	-0.015819
15	53	-0.015657
15	54	-0.015464
15	55	-0.015260
15	56	-0.015059
15	57	-0.014872
15	58	-0.014696
15	59	-0.014522
15	60	-0.014342
15	61	-0.014147
15	62	-0.013928
15	63	-0.013678
15	64	-0.013409
15	65	-0.013136
15	66	-0.012868
15	67	-0.012608
15	68	-0.012364
15	69	-0.012139
15	70	-0.011939
15	71	-0.011770
15	72	-0.011637
15	73	-0.011534
15	74	-0.011448
15	75	-0.011368
15	76	-0.011281
15	77	-0.011175
15	78	-0.011037
15	79	-0.010856
15	80	-0.010618
15	81	-0.010312
15	82	-0.009924
15	83	-0.009444
15	84	-0.008858
15	85	-0.008154
15	86	-0.007319
15	87	-0.006342
15	88	-0.005210
15	89	-0.003911
15	90	-0.002432
25	-10	0
25	30	0
25	31	-0.039513
25	32	-0.044417
25	33	-0.048173
25	34	-0.051173
25	35	-0.054659
25	36	-0.058820
25	37	-0.057986
25	38	-0.054902
25	39	-0.053038
25	40	-0.050733
25	41	-0.048293
25	42	-0.046354
25	43	-0.045126
25	44	-0.044454
25	45	-0.044174
25	46	-0.044122
25	47	-0.044132
25	48	-0.044065
25	49	-0.043893
25	50	-0.043617
25	51	-0.043251
25	52	-0.042819
25	53	-0.042346
25	54	-0.041854
25	55	-0.041356
25	56	-0.040854
25	57	-0.040352
25	58	-0.039854
25	59	-0.039366
25	60	-0.038889
25	61	-0.038427
25	62	-0.037965
25	63	-0.037471
25	64	-0.036935
25	65	-0.036356
25	66	-0.035733
25	67	-0.035065
25	68	-0.034351
25	69	-0.033590
25	70	-0.032783
25	71	-0.031927
25	72	-0.031022
25	73	-0.030067
25	74	-0.029072
25	75	-0.028050
25	76	-0.027013
25	77	-0.025973
25	78	-0.024943
25	79	-0.023935
25	80	-0.022960
25	81	-0.022033
25	82	-0.021164
25	83	-0.020366
25	84	-0.019652
25	85	-0.019033
25	86	-0.018522
25	87	-0.018132
25	88	-0.017874
25	89	-0.017760
25	90	-0.017804

B.3 $C_m(\bar{\delta}_e, \alpha)$

CPMHDE
Increment due to elevon for high aoa, low speed.
020110
2
ALFA
DE

-30	-10	0
-30	30	0
-30	31	0.178350
-30	32	0.177240
-30	33	0.174165
-30	34	0.165199
-30	35	0.146213
-30	36	0.130125
-30	37	0.127900
-30	38	0.131273
-30	39	0.131958
-30	40	0.131245
-30	41	0.129712
-30	42	0.127615
-30	43	0.125248
-30	44	0.122671
-30	45	0.119905
-30	46	0.116972
-30	47	0.113892
-30	48	0.110667
-30	49	0.107287
-30	50	0.103784
-30	51	0.100197
-30	52	0.096561
-30	53	0.092914
-30	54	0.089293
-30	55	0.085750
-30	56	0.082325
-30	57	0.079028
-30	58	0.075868
-30	59	0.072854
-30	60	0.069994
-30	61	0.067298
-30	62	0.064773
-30	63	0.062428
-30	64	0.060250
-30	65	0.058216
-30	66	0.056299
-30	67	0.054473
-30	68	0.052710
-30	69	0.050981
-30	70	0.049260
-30	71	0.047519
-30	72	0.045731
-30	73	0.043880
-30	74	0.041956
-30	75	0.039965
-30	76	0.037930
-30	77	0.035876
-30	78	0.033825
-30	79	0.031802
-30	80	0.029829
-30	81	0.027931
-30	82	0.026131
-30	83	0.024454
-30	84	0.022921
-30	85	0.021558
-30	86	0.020387
-30	87	0.019433
-30	88	0.018720
-30	89	0.018269
-30	90	0.018106
-20	-10	0
-20	30	0
-20	31	0.123518
-20	32	0.122534
-20	33	0.123833
-20	34	0.119197
-20	35	0.103674
-20	36	0.089990
-20	37	0.086181
-20	38	0.087305

-20	39	0.087711
-20	40	0.087811
-20	41	0.087424
-20	42	0.086150
-20	43	0.084019
-20	44	0.081425
-20	45	0.078740
-20	46	0.076132
-20	47	0.073678
-20	48	0.071432
-20	49	0.069334
-20	50	0.067296
-20	51	0.065229
-20	52	0.063054
-20	53	0.060760
-20	54	0.058375
-20	55	0.055937
-20	56	0.053495
-20	57	0.051093
-20	58	0.048778
-20	59	0.046597
-20	60	0.044585
-20	61	0.042752
-20	62	0.041103
-20	63	0.039644
-20	64	0.038361
-20	65	0.037229
-20	66	0.036224
-20	67	0.035321
-20	68	0.034493
-20	69	0.033712
-20	70	0.032950
-20	71	0.032177
-20	72	0.031366
-20	73	0.030498
-20	74	0.029562
-20	75	0.028548
-20	76	0.027453
-20	77	0.026293
-20	78	0.025086
-20	79	0.023848
-20	80	0.022596
-20	81	0.021347
-20	82	0.020119
-20	83	0.018929
-20	84	0.017793
-20	85	0.016730
-20	86	0.015755
-20	87	0.014887
-20	88	0.014142
-20	89	0.013538
-20	90	0.013091
-10	-10	0
-10	30	0
-10	31	0.058748
-10	32	0.057606
-10	33	0.058084
-10	34	0.056108
-10	35	0.046813
-10	36	0.034151
-10	37	0.029976
-10	38	0.031460
-10	39	0.033393
-10	40	0.035714
-10	41	0.037194
-10	42	0.037433
-10	43	0.036549
-10	44	0.035023
-10	45	0.033313
-10	46	0.031635
-10	47	0.030102
-10	48	0.028801
-10	49	0.027709
-10	50	0.026771
-10	51	0.025936
-10	52	0.025155
-10	53	0.024409
-10	54	0.023683
-10	55	0.022974
-10	56	0.022288
-10	57	0.021630
-10	58	0.021003
-10	59	0.020416
-10	60	0.019875
-10	61	0.019390
-10	62	0.018968
-10	63	0.018615
-10	64	0.018320
-10	65	0.018059
-10	66	0.017810
-10	67	0.017550
-10	68	0.017266
-10	69	0.016950
-10	70	0.016595
-10	71	0.016191
-10	72	0.015734
-10	73	0.015225
-10	74	0.014674
-10	75	0.014093
-10	76	0.013490
-10	77	0.012876
-10	78	0.012261
-10	79	0.011653
-10	80	0.011063
-10	81	0.010499
-10	82	0.009972
-10	83	0.009489
-10	84	0.009060
-10	85	0.008696
-10	86	0.008404
-10	87	0.008194
-10	88	0.008076
-10	89	0.008058
-10	90	0.008151
0	-10	0
0	30	0
0	31	0
0	32	0
0	33	0
0	34	0
0	35	0
0	36	0
0	37	0
0	38	0
0	39	0
0	40	0
0	41	0
0	42	0
0	43	0
0	44	0
0	45	0
0	46	0
0	47	0
0	48	0
0	49	0
0	50	0
0	51	0
0	52	0
0	53	0
0	54	0
0	55	0
0	56	0
0	57	0
0	58	0
0	59	0
0	60	0
0	61	0
0	62	0
0	63	0
0	64	0
0	65	0
0	66	0
0	67	0
0	68	0
0	69	0
0	70	0
0	71	0
0	72	0
0	73	0
0	74	0
0	75	0
0	76	0
0	77	0
0	78	0
0	79	0
0	80	0
0	81	0
0	82	0
0	83	0
0	84	0
0	85	0
0	86	0
0	87	0
0	88	0
0	89	0
0	90	0
10	-10	0
10	30	0
10	31	-0.045034
10	32	-0.044982
10	33	-0.044929
10	34	-0.044496
10	35	-0.044332
10	36	-0.044064
10	37	-0.038494
10	38	-0.035024
10	39	-0.037922
10	40	-0.040948
10	41	-0.041636
10	42	-0.040932
10	43	-0.039606
10	44	-0.038062
10	45	-0.036695
10	46	-0.035734
10	47	-0.035052
10	48	-0.034501
10	49	-0.034046
10	50	-0.033679
10	51	-0.033393
10	52	-0.033183
10	53	-0.033042
10	54	-0.032961
10	55	-0.032920
10	56	-0.032895
10	57	-0.032867
10	58	-0.032812
10	59	-0.032710
10	60	-0.032538
10	61	-0.032276
10	62	-0.031901
10	63	-0.031395
10	64	-0.030755
10	65	-0.029991
10	66	-0.029113
10	67	-0.028138
10	68	-0.027083
10	69	-0.025969
10	70	-0.024816
10	71	-0.023643
10	72	-0.022469
10	73	-0.021303
10	74	-0.020147
10	75	-0.019002
10	76	-0.017871
10	77	-0.016756
10	78	-0.015658
10	79	-0.014579
10	80	-0.013521
10	81	-0.012487
10	82	-0.011477
10	83	-0.010494
10	84	-0.009539
10	85	-0.008615
10	86	-0.007724
10	87	-0.006866
10	88	-0.006045
10	89	-0.005262
10	90	-0.004518
20	-10	0
20	30	0
20	31	-0.078705
20	32	-0.080194
20	33	-0.081433

20	34	-0.081848
20	35	-0.081847
20	36	-0.081983
20	37	-0.078927
20	38	-0.076564
20	39	-0.077561
20	40	-0.079299
20	41	-0.081070
20	42	-0.082483
20	43	-0.083043
20	44	-0.082755
20	45	-0.081754
20	46	-0.080178
20	47	-0.078163
20	48	-0.075870
20	49	-0.073572
20	50	-0.071545
20	51	-0.069855
20	52	-0.068462
20	53	-0.067329
20	54	-0.066416
20	55	-0.065671
20	56	-0.065034
20	57	-0.064446
20	58	-0.063848
20	59	-0.063187
20	60	-0.062436
20	61	-0.061579
20	62	-0.060600
20	63	-0.059483
20	64	-0.058233
20	65	-0.056865
20	66	-0.055392
20	67	-0.053829
20	68	-0.052191
20	69	-0.050493
20	70	-0.048748
20	71	-0.046974
20	72	-0.045186
20	73	-0.043394
20	74	-0.041597
20	75	-0.039797
20	76	-0.037995
20	77	-0.036191
20	78	-0.034386
20	79	-0.032582
20	80	-0.030779
20	81	-0.028978
20	82	-0.027179
20	83	-0.025384
20	84	-0.023594
20	85	-0.021808
20	86	-0.020030
20	87	-0.018258
20	88	-0.016494
20	89	-0.014739
20	90	-0.012993
30	-10	0
30	30	0
30	31	-0.098322
30	32	-0.097931
30	33	-0.097048
30	34	-0.096303
30	35	-0.098315
30	36	-0.104134
30	37	-0.106675
30	38	-0.106982
30	39	-0.108116
30	40	-0.108357
30	41	-0.107924
30	42	-0.107357
30	43	-0.106836
30	44	-0.106280
30	45	-0.105606
30	46	-0.104729
30	47	-0.103568
30	48	-0.102064
30	49	-0.100270
30	50	-0.098269
30	51	-0.096144
30	52	-0.093978
30	53	-0.091844
30	54	-0.089768
30	55	-0.087747
30	56	-0.085776
30	57	-0.083848
30	58	-0.081954
30	59	-0.080088
30	60	-0.078242
30	61	-0.076410
30	62	-0.074584
30	63	-0.072756
30	64	-0.070920
30	65	-0.069078
30	66	-0.067233
30	67	-0.065385
30	68	-0.063538
30	69	-0.061692
30	70	-0.059849
30	71	-0.058012
30	72	-0.056182
30	73	-0.054349
30	74	-0.052499
30	75	-0.050622
30	76	-0.048716
30	77	-0.046779
30	78	-0.044809
30	79	-0.042804
30	80	-0.040763
30	81	-0.038683
30	82	-0.036564
30	83	-0.034401
30	84	-0.032195
30	85	-0.029943
30	86	-0.027643
30	87	-0.025294
30	88	-0.022892
30	89	-0.020437
30	90	-0.017927

B.4 $C_N(\bar{\delta}_n, \alpha)$

CNHDN
Increment due to canard for high aoa, low speed.
020110
2
ALFA
DN

-55	-10	0
-55	30	0
-55	31	-0.386308
-55	32	-0.387311
-55	33	-0.384031
-55	34	-0.376300
-55	35	-0.364873
-55	36	-0.350213
-55	37	-0.332789
-55	38	-0.313371
-55	39	-0.293000
-55	40	-0.272725
-55	41	-0.253345
-55	42	-0.235016
-55	43	-0.218125
-55	44	-0.203463
-55	45	-0.191977
-55	46	-0.184625
-55	47	-0.182116
-55	48	-0.183610
-55	49	-0.187647
-55	50	-0.192760
-55	51	-0.197495
-55	52	-0.201039
-55	53	-0.203504
-55	54	-0.205062
-55	55	-0.205886
-55	56	-0.206150
-55	57	-0.206021
-55	58	-0.205552
-55	59	-0.204801
-55	60	-0.203890
-55	61	-0.202942
-55	62	-0.202078
-55	63	-0.201422
-55	64	-0.201082
-55	65	-0.201046
-55	66	-0.201233
-55	67	-0.201555
-55	68	-0.201924
-55	69	-0.202252
-55	70	-0.202454
-55	71	-0.202492
-55	72	-0.202420
-55	73	-0.202302
-55	74	-0.202179
-55	75	-0.202057
-55	76	-0.201938
-55	77	-0.201824
-55	78	-0.201716
-55	79	-0.201618
-55	80	-0.201531
-55	81	-0.201457
-55	82	-0.201399
-55	83	-0.201359
-55	84	-0.201339
-55	85	-0.201342
-55	86	-0.201368
-55	87	-0.201421
-55	88	-0.201503
-55	89	-0.201615
-55	90	-0.201761
-45	-10	0
-45	30	0
-45	31	-0.353080
-45	32	-0.352945
-45	33	-0.350057
-45	34	-0.344632
-45	35	-0.336313
-45	36	-0.324378
-45	37	-0.308312
-45	38	-0.289091
-45	39	-0.268456
-45	40	-0.248157
-45	41	-0.229694
-45	42	-0.213834
-45	43	-0.200727
-45	44	-0.190405
-45	45	-0.183043
-45	46	-0.178759
-45	47	-0.177279
-45	48	-0.177864
-45	49	-0.179581
-45	50	-0.181826
-45	51	-0.184323
-45	52	-0.186810
-45	53	-0.189019
-45	54	-0.190687
-45	55	-0.191697
-45	56	-0.192014
-45	57	-0.191605
-45	58	-0.190460
-45	59	-0.188741
-45	60	-0.186679
-45	61	-0.184510
-45	62	-0.182466
-45	63	-0.180783
-45	64	-0.179635
-45	65	-0.178996
-45	66	-0.178761
-45	67	-0.178827
-45	68	-0.179088

-45	69	-0.179441
-45	70	-0.179783
-45	71	-0.180059
-45	72	-0.180308
-45	73	-0.180577
-45	74	-0.180890
-45	75	-0.181235
-45	76	-0.181599
-45	77	-0.181967
-45	78	-0.182324
-45	79	-0.182656
-45	80	-0.182949
-45	81	-0.183187
-45	82	-0.183358
-45	83	-0.183445
-45	84	-0.183435
-45	85	-0.183313
-45	86	-0.183065
-45	87	-0.182677
-45	88	-0.182133
-45	89	-0.181420
-45	90	-0.180522
-35	-10	0
-35	30	0
-35	31	-0.299789
-35	32	-0.303642
-35	33	-0.303683
-35	34	-0.298496
-35	35	-0.289247
-35	36	-0.276990
-35	37	-0.262654
-35	38	-0.247200
-35	39	-0.231947
-35	40	-0.218194
-35	41	-0.206695
-35	42	-0.197358
-35	43	-0.189946
-35	44	-0.184131
-35	45	-0.179676
-35	46	-0.176465
-35	47	-0.174559
-35	48	-0.173699
-35	49	-0.173420
-35	50	-0.173257
-35	51	-0.172945
-35	52	-0.172500
-35	53	-0.171957
-35	54	-0.171338
-35	55	-0.170666
-35	56	-0.169962
-35	57	-0.169223
-35	58	-0.168346
-35	59	-0.167362
-35	60	-0.166375
-35	61	-0.165488
-35	62	-0.164806
-35	63	-0.164433
-35	64	-0.164459
-35	65	-0.164855
-35	66	-0.165523
-35	67	-0.166363
-35	68	-0.167279
-35	69	-0.168170
-35	70	-0.168941
-35	71	-0.169542
-35	72	-0.170018
-35	73	-0.170422
-35	74	-0.170784
-35	75	-0.171098
-35	76	-0.171356
-35	77	-0.171550
-35	78	-0.171670
-35	79	-0.171709
-35	80	-0.171657
-35	81	-0.171507
-35	82	-0.171248
-35	83	-0.170874
-35	84	-0.170375
-35	85	-0.169743
-35	86	-0.168968
-35	87	-0.168044
-35	88	-0.166960
-35	89	-0.165709
-35	90	-0.164281
-25	-10	0
-25	30	0
-25	31	-0.219455
-25	32	-0.221785
-25	33	-0.221233
-25	34	-0.215883
-25	35	-0.207329
-25	36	-0.197899
-25	37	-0.189289
-25	38	-0.180967
-25	39	-0.172135
-25	40	-0.162430
-25	41	-0.153233
-25	42	-0.145846
-25	43	-0.140898
-25	44	-0.138172
-25	45	-0.137501
-25	46	-0.138586
-25	47	-0.140720
-25	48	-0.142799
-25	49	-0.143633
-25	50	-0.143099
-25	51	-0.141621
-25	52	-0.139630
-25	53	-0.137548
-25	54	-0.135788
-25	55	-0.134580
-25	56	-0.133757
-25	57	-0.133098
-25	58	-0.132410
-25	59	-0.131666
-25	60	-0.130914
-25	61	-0.130202
-25	62	-0.129579
-25	63	-0.129116
-25	64	-0.128918
-25	65	-0.128968
-25	66	-0.129186
-25	67	-0.129489
-25	68	-0.129795
-25	69	-0.130022
-25	70	-0.130088
-25	71	-0.129961
-25	72	-0.129703
-25	73	-0.129381
-25	74	-0.129042
-25	75	-0.128697
-25	76	-0.128354
-25	77	-0.128020
-25	78	-0.127702
-25	79	-0.127409
-25	80	-0.127147
-25	81	-0.126925
-25	82	-0.126750
-25	83	-0.126629
-25	84	-0.126570
-25	85	-0.126581
-25	86	-0.126670
-25	87	-0.126843
-25	88	-0.127108
-25	89	-0.127474
-25	90	-0.127947
-15	-10	0
-15	30	0
-15	31	-0.138239
-15	32	-0.142453
-15	33	-0.144471
-15	34	-0.142297
-15	35	-0.136752
-15	36	-0.128806
-15	37	-0.119491
-15	38	-0.110387
-15	39	-0.102262
-15	40	-0.095485
-15	41	-0.090252
-15	42	-0.086326
-15	43	-0.083413
-15	44	-0.081321
-15	45	-0.080028
-15	46	-0.079656
-15	47	-0.080351
-15	48	-0.081919
-15	49	-0.084005
-15	50	-0.086397
-15	51	-0.088914
-15	52	-0.091376
-15	53	-0.093608
-15	54	-0.095501
-15	55	-0.096977
-15	56	-0.097958
-15	57	-0.098367
-15	58	-0.098149
-15	59	-0.097419
-15	60	-0.096355
-15	61	-0.095110
-15	62	-0.093840
-15	63	-0.092698
-15	64	-0.091825
-15	65	-0.091240
-15	66	-0.090895
-15	67	-0.090742
-15	68	-0.090731
-15	69	-0.090792
-15	70	-0.090828
-15	71	-0.090792
-15	72	-0.090728
-15	73	-0.090687
-15	74	-0.090699
-15	75	-0.090760
-15	76	-0.090859
-15	77	-0.090989
-15	78	-0.091140
-15	79	-0.091303
-15	80	-0.091470
-15	81	-0.091631
-15	82	-0.091779
-15	83	-0.091903
-15	84	-0.091995
-15	85	-0.092046
-15	86	-0.092047
-15	87	-0.091990
-15	88	-0.091865
-15	89	-0.091664
-15	90	-0.091377
-5	-10	0
-5	30	0
-5	31	-0.043895
-5	32	-0.041118
-5	33	-0.038842
-5	34	-0.037893
-5	35	-0.037473
-5	36	-0.036292
-5	37	-0.033146
-5	38	-0.028104
-5	39	-0.022193
-5	40	-0.016464
-5	41	-0.011718
-5	42	-0.008066
-5	43	-0.005359
-5	44	-0.003492
-5	45	-0.002511
-5	46	-0.002470
-5	47	-0.003393
-5	48	-0.005020
-5	49	-0.007133
-5	50	-0.009579
-5	51	-0.012201
-5	52	-0.014847
-5	53	-0.017355
-5	54	-0.019555
-5	55	-0.021286
-5	56	-0.022457
-5	57	-0.023001
-5	58	-0.022875
-5	59	-0.022205
-5	60	-0.021192
-5	61	-0.020036
-5	62	-0.018937
-5	63	-0.018065

-5	64	-0.017528
-5	65	-0.017305
-5	66	-0.017311
-5	67	-0.017458
-5	68	-0.017660
-5	69	-0.017830
-5	70	-0.017882
-5	71	-0.017779
-5	72	-0.017577
-5	73	-0.017340
-5	74	-0.017110
-5	75	-0.016892
-5	76	-0.016691
-5	77	-0.016508
-5	78	-0.016347
-5	79	-0.016210
-5	80	-0.016101
-5	81	-0.016021
-5	82	-0.015975
-5	83	-0.015965
-5	84	-0.015994
-5	85	-0.016064
-5	86	-0.016180
-5	87	-0.016342
-5	88	-0.016556
-5	89	-0.016822
-5	90	-0.017145
0	-10	0
0	30	0
0	31	0
0	32	0
0	33	0
0	34	0
0	35	0
0	36	0
0	37	0
0	38	0
0	39	0
0	40	0
0	41	0
0	42	0
0	43	0
0	44	0
0	45	0
0	46	0
0	47	0
0	48	0
0	49	0
0	50	0
0	51	0
0	52	0
0	53	0
0	54	0
0	55	0
0	56	0
0	57	0
0	58	0
0	59	0
0	60	0
0	61	0
0	62	0
0	63	0
0	64	0
0	65	0
0	66	0
0	67	0
0	68	0
0	69	0
0	70	0
0	71	0
0	72	0
0	73	0
0	74	0
0	75	0
0	76	0
0	77	0
0	78	0
0	79	0
0	80	0
0	81	0
0	82	0

0	83	0
0	84	0
0	85	0
0	86	0
0	87	0
0	88	0
0	89	0
0	90	0
5	-10	0
5	30	0
5	31	0.001329
5	32	0.000872
5	33	0.000445
5	34	-0.000119
5	35	-0.001079
5	36	-0.002515
5	37	-0.004121
5	38	-0.005284
5	39	-0.005799
5	40	-0.005857
5	41	-0.006081
5	42	-0.006500
5	43	-0.007034
5	44	-0.007670
5	45	-0.008486
5	46	-0.009566
5	47	-0.010964
5	48	-0.012391
5	49	-0.013427
5	50	-0.014025
5	51	-0.014258
5	52	-0.014202
5	53	-0.013923
5	54	-0.013480
5	55	-0.012930
5	56	-0.012329
5	57	-0.011649
5	58	-0.010764
5	59	-0.009708
5	60	-0.008590
5	61	-0.007518
5	62	-0.006600
5	63	-0.005945
5	64	-0.005649
5	65	-0.005684
5	66	-0.005957
5	67	-0.006375
5	68	-0.006843
5	69	-0.007272
5	70	-0.007574
5	71	-0.007711
5	72	-0.007736
5	73	-0.007711
5	74	-0.007676
5	75	-0.007636
5	76	-0.007591
5	77	-0.007542
5	78	-0.007490
5	79	-0.007436
5	80	-0.007380
5	81	-0.007325
5	82	-0.007270
5	83	-0.007216
5	84	-0.007165
5	85	-0.007118
5	86	-0.007074
5	87	-0.007036
5	88	-0.007004
5	89	-0.006979
5	90	-0.006962
15	-10	0
15	30	0
15	31	-0.019096
15	32	-0.017862
15	33	-0.017611
15	34	-0.019721
15	35	-0.023885
15	36	-0.029100
15	37	-0.034354
15	38	-0.039193
15	39	-0.043681

15	40	-0.047912
15	41	-0.051876
15	42	-0.054958
15	43	-0.056439
15	44	-0.055933
15	45	-0.053991
15	46	-0.051344
15	47	-0.048689
15	48	-0.046387
15	49	-0.044589
15	50	-0.043398
15	51	-0.042737
15	52	-0.042484
15	53	-0.042512
15	54	-0.042683
15	55	-0.042859
15	56	-0.042900
15	57	-0.042670
15	58	-0.042051
15	59	-0.041093
15	60	-0.039919
15	61	-0.038655
15	62	-0.037422
15	63	-0.036344
15	64	-0.035533
15	65	-0.034977
15	66	-0.034597
15	67	-0.034316
15	68	-0.034053
15	69	-0.033730
15	70	-0.033269
15	71	-0.032641
15	72	-0.031911
15	73	-0.031150
15	74	-0.030407
15	75	-0.029699
15	76	-0.029034
15	77	-0.028424
15	78	-0.027880
15	79	-0.027413
15	80	-0.027033
15	81	-0.026752
15	82	-0.026581
15	83	-0.026530
15	84	-0.026610
15	85	-0.026832
15	86	-0.027208
15	87	-0.027748
15	88	-0.028463
15	89	-0.029363
15	90	-0.030461
25	-10	0
25	30	0
25	31	-0.074424
25	32	-0.084076
25	33	-0.092115
25	34	-0.099491
25	35	-0.106937
25	36	-0.113721
25	37	-0.118464
25	38	-0.120618
25	39	-0.120219
25	40	-0.117616
25	41	-0.113720
25	42	-0.108916
25	43	-0.103482
25	44	-0.097773
25	45	-0.092202
25	46	-0.087176
25	47	-0.083067
25	48	-0.079909
25	49	-0.077531
25	50	-0.075756
25	51	-0.074409
25	52	-0.073347
25	53	-0.072474
25	54	-0.071686
25	55	-0.070879
25	56	-0.069948
25	57	-0.068790
25	58	-0.067324

25	59	-0.065639
25	60	-0.063899
25	61	-0.062248
25	62	-0.060799
25	63	-0.059662
25	64	-0.058934
25	65	-0.058589
25	66	-0.058534
25	67	-0.058676
25	68	-0.058923
25	69	-0.059182
25	70	-0.059360
25	71	-0.059416
25	72	-0.059397
25	73	-0.059363
25	74	-0.059349
25	75	-0.059355
25	76	-0.059379
25	77	-0.059416
25	78	-0.059463
25	79	-0.059518
25	80	-0.059577
25	81	-0.059638
25	82	-0.059696
25	83	-0.059748
25	84	-0.059792
25	85	-0.059824
25	86	-0.059842
25	87	-0.059841
25	88	-0.059819
25	89	-0.059772
25	90	-0.059697

B.5 $C_N(\bar{\delta}_e, \alpha)$

CNHDE
Increment due to elevon for high aoa, low speed.
020110
2
DE
ALFA

-30	-10	0
-30	30	0
-30	31	-0.454683
-30	32	-0.448585
-30	33	-0.440114
-30	34	-0.429626
-30	35	-0.418693
-30	36	-0.407909
-30	37	-0.396536
-30	38	-0.384485
-30	39	-0.372250
-30	40	-0.360475
-30	41	-0.350015
-30	42	-0.341162
-30	43	-0.334100
-30	44	-0.329062
-30	45	-0.325927
-30	46	-0.324303
-30	47	-0.323764
-30	48	-0.323555
-30	49	-0.323129
-30	50	-0.322493
-30	51	-0.321692
-30	52	-0.320771
-30	53	-0.319770
-30	54	-0.318714
-30	55	-0.317549
-30	56	-0.316122
-30	57	-0.314279
-30	58	-0.311887
-30	59	-0.308984
-30	60	-0.305680
-30	61	-0.302095
-30	62	-0.298376
-30	63	-0.294681
-30	64	-0.291153
-30	65	-0.287815
-30	66	-0.284620
-30	67	-0.281523
-30	68	-0.278478
-30	69	-0.275438
-30	70	-0.272341
-30	71	-0.269145
-30	72	-0.265897
-30	73	-0.262652
-30	74	-0.259444
-30	75	-0.256271
-30	76	-0.253127
-30	77	-0.250007
-30	78	-0.246906
-30	79	-0.243819
-30	80	-0.240743
-30	81	-0.237677
-30	82	-0.234619
-30	83	-0.231565
-30	84	-0.228514
-30	85	-0.225463
-30	86	-0.222411
-30	87	-0.219355
-30	88	-0.216293
-30	89	-0.213222
-30	90	-0.210140
-20	-10	0
-20	30	0
-20	31	-0.310719
-20	32	-0.307891
-20	33	-0.305765
-20	34	-0.304273
-20	35	-0.302835
-20	36	-0.300501
-20	37	-0.296456
-20	38	-0.290798
-20	39	-0.284212
-20	40	-0.277393
-20	41	-0.270787
-20	42	-0.264183
-20	43	-0.257487
-20	44	-0.250977
-20	45	-0.245091
-20	46	-0.240278
-20	47	-0.236957
-20	48	-0.235206
-20	49	-0.234895
-20	50	-0.235890
-20	51	-0.237922
-20	52	-0.240588
-20	53	-0.243468
-20	54	-0.246135
-20	55	-0.248161
-20	56	-0.249115
-20	57	-0.248569
-20	58	-0.246167
-20	59	-0.242075
-20	60	-0.236682
-20	61	-0.230380
-20	62	-0.223559
-20	63	-0.216611
-20	64	-0.209915
-20	65	-0.203726
-20	66	-0.198233
-20	67	-0.193589
-20	68	-0.189712
-20	69	-0.186423
-20	70	-0.183546
-20	71	-0.180956
-20	72	-0.178616
-20	73	-0.176501
-20	74	-0.174563
-20	75	-0.172716
-20	76	-0.170874
-20	77	-0.168949
-20	78	-0.166892
-20	79	-0.164750
-20	80	-0.162586
-20	81	-0.160461
-20	82	-0.158438
-20	83	-0.156580
-20	84	-0.154948
-20	85	-0.153605
-20	86	-0.152613
-20	87	-0.152034
-20	88	-0.151932
-20	89	-0.152367
-20	90	-0.153402
-10	-10	0
-10	30	0
-10	31	-0.153688
-10	32	-0.157022
-10	33	-0.160283
-10	34	-0.163558
-10	35	-0.166788
-10	36	-0.169566
-10	37	-0.171551
-10	38	-0.173244
-10	39	-0.175469
-10	40	-0.178216
-10	41	-0.181047
-10	42	-0.182867
-10	43	-0.182929
-10	44	-0.181517
-10	45	-0.179171
-10	46	-0.176444
-10	47	-0.173854
-10	48	-0.171572
-10	49	-0.169557
-10	50	-0.167760
-10	51	-0.166137
-10	52	-0.164639
-10	53	-0.163214
-10	54	-0.161796
-10	55	-0.160265
-10	56	-0.158469
-10	57	-0.156253
-10	58	-0.153486
-10	59	-0.150209
-10	60	-0.146533
-10	61	-0.142573
-10	62	-0.138440
-10	63	-0.134249
-10	64	-0.130100
-10	65	-0.126008
-10	66	-0.121956
-10	67	-0.117930
-10	68	-0.113916
-10	69	-0.109900
-10	70	-0.105867
-10	71	-0.101855
-10	72	-0.097990
-10	73	-0.094410
-10	74	-0.091200
-10	75	-0.088338
-10	76	-0.085791
-10	77	-0.083525
-10	78	-0.081508
-10	79	-0.079706
-10	80	-0.078085
-10	81	-0.076612
-10	82	-0.075253
-10	83	-0.073975
-10	84	-0.072745
-10	85	-0.071529
-10	86	-0.070294
-10	87	-0.069006
-10	88	-0.067631
-10	89	-0.066138
-10	90	-0.064491
0	-10	0
0	30	0
0	31	0

0	32	0
0	33	0
0	34	0
0	35	0
0	36	0
0	37	0
0	38	0
0	39	0
0	40	0
0	41	0
0	42	0
0	43	0
0	44	0
0	45	0
0	46	0
0	47	0
0	48	0
0	49	0
0	50	0
0	51	0
0	52	0
0	53	0
0	54	0
0	55	0
0	56	0
0	57	0
0	58	0
0	59	0
0	60	0
0	61	0
0	62	0
0	63	0
0	64	0
0	65	0
0	66	0
0	67	0
0	68	0
0	69	0
0	70	0
0	71	0
0	72	0
0	73	0
0	74	0
0	75	0
0	76	0
0	77	0
0	78	0
0	79	0
0	80	0
0	81	0
0	82	0
0	83	0
0	84	0
0	85	0
0	86	0
0	87	0
0	88	0
0	89	0
0	90	0
10	-10	0
10	30	0
10	31	0.106912
10	32	0.094250
10	33	0.083848
10	34	0.074434
10	35	0.065283
10	36	0.056031
10	37	0.046515
10	38	0.037252
10	39	0.028719
10	40	0.021381
10	41	0.015636
10	42	0.011727
10	43	0.009878
10	44	0.010206
10	45	0.012678
10	46	0.016923
10	47	0.022069
10	48	0.027531
10	49	0.032933
10	50	0.037903
10	51	0.042065
10	52	0.045051
10	53	0.046698
10	54	0.047250
10	55	0.046990
10	56	0.046206
10	57	0.045183
10	58	0.044184
10	59	0.043301
10	60	0.042552
10	61	0.041957
10	62	0.041482
10	63	0.041002
10	64	0.040398
10	65	0.039671
10	66	0.038890
10	67	0.038125
10	68	0.037443
10	69	0.036916
10	70	0.036612
10	71	0.036548
10	72	0.036652
10	73	0.036843
10	74	0.037060
10	75	0.037280
10	76	0.037483
10	77	0.037648
10	78	0.037754
10	79	0.037782
10	80	0.037710
10	81	0.037518
10	82	0.037186
10	83	0.036692
10	84	0.036017
10	85	0.035141
10	86	0.034041
10	87	0.032699
10	88	0.031093
10	89	0.029203
10	90	0.027009
20	-10	0
20	30	0
20	31	0.171066
20	32	0.155160
20	33	0.142467
20	34	0.131337
20	35	0.118194
20	36	0.099865
20	37	0.076972
20	38	0.056094
20	39	0.041362
20	40	0.032149
20	41	0.027568
20	42	0.027341
20	43	0.030813
20	44	0.036970
20	45	0.044647
20	46	0.052669
20	47	0.059917
20	48	0.065969
20	49	0.070890
20	50	0.074755
20	51	0.077639
20	52	0.079617
20	53	0.080770
20	54	0.081191
20	55	0.081027
20	56	0.080484
20	57	0.079775
20	58	0.079085
20	59	0.078433
20	60	0.077763
20	61	0.077018
20	62	0.076141
20	63	0.075077
20	64	0.073783
20	65	0.072336
20	66	0.070882
20	67	0.069557
20	68	0.068438
20	69	0.067587
20	70	0.067066
20	71	0.066885
20	72	0.066965
20	73	0.067216
20	74	0.067571
20	75	0.067999
20	76	0.068473
20	77	0.068964
20	78	0.069445
20	79	0.069887
20	80	0.070264
20	81	0.070546
20	82	0.070706
20	83	0.070717
20	84	0.070549
20	85	0.070176
20	86	0.069569
20	87	0.068701
20	88	0.067544
20	89	0.066069
20	90	0.064249
30	-10	0
30	30	0
30	31	0.193986
30	32	0.172756
30	33	0.151140
30	34	0.128721
30	35	0.105847
30	36	0.084192
30	37	0.066117
30	38	0.053157
30	39	0.045763
30	40	0.042714
30	41	0.042703
30	42	0.045087
30	43	0.049329
30	44	0.054786
30	45	0.060702
30	46	0.066475
30	47	0.071590
30	48	0.075867
30	49	0.079336
30	50	0.082030
30	51	0.083981
30	52	0.085231
30	53	0.085904
30	54	0.086171
30	55	0.086204
30	56	0.086175
30	57	0.086257
30	58	0.086598
30	59	0.087177
30	60	0.087899
30	61	0.088670
30	62	0.089393
30	63	0.089971
30	64	0.090298
30	65	0.090380
30	66	0.090292
30	67	0.090111
30	68	0.089910
30	69	0.089766
30	70	0.089753
30	71	0.089896
30	72	0.090128
30	73	0.090372
30	74	0.090576
30	75	0.090721
30	76	0.090794
30	77	0.090780
30	78	0.090665
30	79	0.090433
30	80	0.090070
30	81	0.089563
30	82	0.088896
30	83	0.088056
30	84	0.087026
30	85	0.085794
30	86	0.084344
30	87	0.082663
30	88	0.080735

30	89	0.078546
30	90	0.076081

B.6 $C_T(\bar{\delta}_n, \alpha)$

CTHDN
Increment due to canard for high aoa, low speed.
020110
2
ALFA
DN

-55	-10	0
-55	30	0
-55	31	0.086591
-55	32	0.084046
-55	33	0.082196
-55	34	0.080641
-55	35	0.079125
-55	36	0.077668
-55	37	0.076318
-55	38	0.075099
-55	39	0.073964
-55	40	0.072850
-55	41	0.071723
-55	42	0.070632
-55	43	0.069662
-55	44	0.068857
-55	45	0.068164
-55	46	0.067513
-55	47	0.066856
-55	48	0.066219
-55	49	0.065650
-55	50	0.065196
-55	51	0.064888
-55	52	0.064728
-55	53	0.064709
-55	54	0.064828
-55	55	0.065080
-55	56	0.065460
-55	57	0.065957
-55	58	0.066558
-55	59	0.067246
-55	60	0.068009
-55	61	0.068832
-55	62	0.069701
-55	63	0.070603
-55	64	0.071522
-55	65	0.072447
-55	66	0.073365
-55	67	0.074268
-55	68	0.075153
-55	69	0.076018
-55	70	0.076861
-55	71	0.077681
-55	72	0.078476
-55	73	0.079245
-55	74	0.079985
-55	75	0.080696
-55	76	0.081374
-55	77	0.082020
-55	78	0.082630
-55	79	0.083204
-55	80	0.083740
-55	81	0.084236
-55	82	0.084690
-55	83	0.085103
-55	84	0.085476
-55	85	0.085810
-55	86	0.086106
-55	87	0.086365
-55	88	0.086589
-55	89	0.086778
-55	90	0.086935
-45	-10	0
-45	30	0
-45	31	0.025766
-45	32	0.022648
-45	33	0.021378
-45	34	0.020582
-45	35	0.019345
-45	36	0.017720
-45	37	0.015886
-45	38	0.013998
-45	39	0.012139
-45	40	0.010377
-45	41	0.008798
-45	42	0.007564
-45	43	0.006795
-45	44	0.006481
-45	45	0.006511
-45	46	0.006754
-45	47	0.007103
-45	48	0.007507
-45	49	0.007926
-45	50	0.008319
-45	51	0.008666
-45	52	0.008973
-45	53	0.009251
-45	54	0.009509
-45	55	0.009756
-45	56	0.010003
-45	57	0.010260
-45	58	0.010539
-45	59	0.010855
-45	60	0.011222
-45	61	0.011656
-45	62	0.012169
-45	63	0.012764
-45	64	0.013430
-45	65	0.014157
-45	66	0.014939
-45	67	0.015768
-45	68	0.016639
-45	69	0.017544
-45	70	0.018477
-45	71	0.019430
-45	72	0.020397
-45	73	0.021372
-45	74	0.022347
-45	75	0.023315
-45	76	0.024271
-45	77	0.025206
-45	78	0.026115
-45	79	0.026991
-45	80	0.027827
-45	81	0.028615
-45	82	0.029350
-45	83	0.030027
-45	84	0.030641
-45	85	0.031189
-45	86	0.031666
-45	87	0.032070
-45	88	0.032395
-45	89	0.032638
-45	90	0.032795
-35	-10	0
-35	30	0
-35	31	-0.015505
-35	32	-0.020383
-35	33	-0.024331
-35	34	-0.027625
-35	35	-0.030474
-35	36	-0.032972
-35	37	-0.035203
-35	38	-0.037276
-35	39	-0.039373
-35	40	-0.041624
-35	41	-0.044023
-35	42	-0.046469
-35	43	-0.048831
-35	44	-0.051014
-35	45	-0.053024
-35	46	-0.054882
-35	47	-0.056590
-35	48	-0.058094
-35	49	-0.059347
-35	50	-0.060309
-35	51	-0.060951
-35	52	-0.061278
-35	53	-0.061301
-35	54	-0.061029
-35	55	-0.060472
-35	56	-0.059638
-35	57	-0.058545
-35	58	-0.057215
-35	59	-0.055672
-35	60	-0.053937
-35	61	-0.052035
-35	62	-0.049988
-35	63	-0.047818
-35	64	-0.045549
-35	65	-0.043203
-35	66	-0.040795
-35	67	-0.038327
-35	68	-0.035798
-35	69	-0.033206
-35	70	-0.030551
-35	71	-0.027830
-35	72	-0.025044
-35	73	-0.022189
-35	74	-0.019266
-35	75	-0.016283
-35	76	-0.013270
-35	77	-0.010258
-35	78	-0.007278
-35	79	-0.004360
-35	80	-0.001536
-35	81	0.001163
-35	82	0.003707
-35	83	0.006067
-35	84	0.008213
-35	85	0.010119
-35	86	0.011756
-35	87	0.013096
-35	88	0.014110
-35	89	0.014771
-35	90	0.015051
-25	-10	0
-25	30	0
-25	31	-0.033904
-25	32	-0.035657
-25	33	-0.036941
-25	34	-0.038199
-25	35	-0.039753
-25	36	-0.041553
-25	37	-0.043452
-25	38	-0.045330
-25	39	-0.047137
-25	40	-0.048837
-25	41	-0.050380
-25	42	-0.051631
-25	43	-0.052429
-25	44	-0.052680
-25	45	-0.052482
-25	46	-0.051966
-25	47	-0.051241
-25	48	-0.050360
-25	49	-0.049363
-25	50	-0.048292
-25	51	-0.047183
-25	52	-0.046038
-25	53	-0.044850
-25	54	-0.043614
-25	55	-0.042321
-25	56	-0.040966
-25	57	-0.039542
-25	58	-0.038038
-25	59	-0.036442
-25	60	-0.034744
-25	61	-0.032936

-25	62	-0.031037
-25	63	-0.029067
-25	64	-0.027050
-25	65	-0.025008
-25	66	-0.022959
-25	67	-0.020924
-25	68	-0.018920
-25	69	-0.016955
-25	70	-0.015018
-25	71	-0.013098
-25	72	-0.011185
-25	73	-0.009268
-25	74	-0.007337
-25	75	-0.005382
-25	76	-0.003391
-25	77	-0.001375
-25	78	0.000630
-25	79	0.002585
-25	80	0.004450
-25	81	0.006186
-25	82	0.007754
-25	83	0.009116
-25	84	0.010236
-25	85	0.011079
-25	86	0.011606
-25	87	0.011783
-25	88	0.011573
-25	89	0.010938
-25	90	0.009844
-15	-10	0
-15	30	0
-15	31	-0.030072
-15	32	-0.030497
-15	33	-0.030704
-15	34	-0.030889
-15	35	-0.031142
-15	36	-0.031412
-15	37	-0.031636
-15	38	-0.031779
-15	39	-0.031876
-15	40	-0.031976
-15	41	-0.032113
-15	42	-0.032230
-15	43	-0.032239
-15	44	-0.032083
-15	45	-0.031809
-15	46	-0.031478
-15	47	-0.031131
-15	48	-0.030752
-15	49	-0.030309
-15	50	-0.029765
-15	51	-0.029091
-15	52	-0.028294
-15	53	-0.027383
-15	54	-0.026368
-15	55	-0.025258
-15	56	-0.024064
-15	57	-0.022793
-15	58	-0.021454
-15	59	-0.020054
-15	60	-0.018606
-15	61	-0.017121
-15	62	-0.015613
-15	63	-0.014092
-15	64	-0.012572
-15	65	-0.011063
-15	66	-0.009576
-15	67	-0.008117
-15	68	-0.006698
-15	69	-0.005326
-15	70	-0.004009
-15	71	-0.002741
-15	72	-0.001512
-15	73	-0.000309
-15	74	0.000880
-15	75	0.002068
-15	76	0.003266
-15	77	0.004487
-15	78	0.005743
-15	79	0.007036
-15	80	0.008343
-15	81	0.009630
-15	82	0.010866
-15	83	0.012020
-15	84	0.013063
-15	85	0.013966
-15	86	0.014699
-15	87	0.015234
-15	88	0.015541
-15	89	0.015590
-15	90	0.015354
-5	-10	0
-5	30	0
-5	31	-0.009258
-5	32	-0.008858
-5	33	-0.008458
-5	34	-0.008231
-5	35	-0.008258
-5	36	-0.008445
-5	37	-0.008679
-5	38	-0.008872
-5	39	-0.009005
-5	40	-0.009075
-5	41	-0.009073
-5	42	-0.008947
-5	43	-0.008627
-5	44	-0.008079
-5	45	-0.007370
-5	46	-0.006583
-5	47	-0.005780
-5	48	-0.004962
-5	49	-0.004122
-5	50	-0.003248
-5	51	-0.002347
-5	52	-0.001457
-5	53	-0.000620
-5	54	0.000121
-5	55	0.000726
-5	56	0.001182
-5	57	0.001507
-5	58	0.001720
-5	59	0.001842
-5	60	0.001894
-5	61	0.001899
-5	62	0.001878
-5	63	0.001852
-5	64	0.001842
-5	65	0.001868
-5	66	0.001935
-5	67	0.002038
-5	68	0.002176
-5	69	0.002346
-5	70	0.002545
-5	71	0.002770
-5	72	0.003020
-5	73	0.003291
-5	74	0.003580
-5	75	0.003885
-5	76	0.004197
-5	77	0.004507
-5	78	0.004805
-5	79	0.005081
-5	80	0.005326
-5	81	0.005531
-5	82	0.005685
-5	83	0.005781
-5	84	0.005812
-5	85	0.005771
-5	86	0.005652
-5	87	0.005447
-5	88	0.005150
-5	89	0.004755
-5	90	0.004254
0	-10	0
0	30	0
0	31	0
0	32	0
0	33	0
0	34	0
0	35	0
0	36	0
0	37	0
0	38	0
0	39	0
0	40	0
0	41	0
0	42	0
0	43	0
0	44	0
0	45	0
0	46	0
0	47	0
0	48	0
0	49	0
0	50	0
0	51	0
0	52	0
0	53	0
0	54	0
0	55	0
0	56	0
0	57	0
0	58	0
0	59	0
0	60	0
0	61	0
0	62	0
0	63	0
0	64	0
0	65	0
0	66	0
0	67	0
0	68	0
0	69	0
0	70	0
0	71	0
0	72	0
0	73	0
0	74	0
0	75	0
0	76	0
0	77	0
0	78	0
0	79	0
0	80	0
0	81	0
0	82	0
0	83	0
0	84	0
0	85	0
0	86	0
0	87	0
0	88	0
0	89	0
0	90	0
5	-10	0
5	30	0
5	31	0.021697
5	32	0.022544
5	33	0.023509
5	34	0.024294
5	35	0.024687
5	36	0.024719
5	37	0.024507
5	38	0.024145
5	39	0.023656
5	40	0.023047
5	41	0.022341
5	42	0.021643
5	43	0.021055
5	44	0.020629
5	45	0.020320
5	46	0.020061
5	47	0.019811
5	48	0.019583
5	49	0.019404
5	50	0.019297
5	51	0.019273
5	52	0.019311
5	53	0.019383
5	54	0.019477
5	55	0.019588
5	56	0.019711

5	57	0.019841
5	58	0.019978
5	59	0.020121
5	60	0.020270
5	61	0.020426
5	62	0.020589
5	63	0.020758
5	64	0.020934
5	65	0.021119
5	66	0.021314
5	67	0.021524
5	68	0.021749
5	69	0.021983
5	70	0.022220
5	71	0.022455
5	72	0.022683
5	73	0.022897
5	74	0.023092
5	75	0.023263
5	76	0.023403
5	77	0.023507
5	78	0.023569
5	79	0.023584
5	80	0.023546
5	81	0.023449
5	82	0.023288
5	83	0.023059
5	84	0.022759
5	85	0.022386
5	86	0.021935
5	87	0.021406
5	88	0.020794
5	89	0.020097
5	90	0.019313
15	-10	0
15	30	0
15	31	0.065940
15	32	0.066732
15	33	0.067599
15	34	0.068199
15	35	0.068349
15	36	0.068129
15	37	0.067642
15	38	0.066967
15	39	0.066110
15	40	0.065065
15	41	0.063840
15	42	0.062525
15	43	0.061241
15	44	0.060071
15	45	0.058989
15	46	0.057945
15	47	0.056908
15	48	0.055908
15	49	0.054983
15	50	0.054173
15	51	0.053500
15	52	0.052958
15	53	0.052532
15	54	0.052209
15	55	0.051978
15	56	0.051825
15	57	0.051738
15	58	0.051709
15	59	0.051730
15	60	0.051793
15	61	0.051890
15	62	0.052015
15	63	0.052160
15	64	0.052318
15	65	0.052481
15	66	0.052645
15	67	0.052806
15	68	0.052960
15	69	0.053099
15	70	0.053217
15	71	0.053307
15	72	0.053362
15	73	0.053374
15	74	0.053337
15	75	0.053244
15	76	0.053087
15	77	0.052860
15	78	0.052555
15	79	0.052166
15	80	0.051686
15	81	0.051107
15	82	0.050423
15	83	0.049628
15	84	0.048719
15	85	0.047691
15	86	0.046539
15	87	0.045260
15	88	0.043850
15	89	0.042305
15	90	0.040619
25	-10	0
25	30	0
25	31	0.102194
25	32	0.102143
25	33	0.102038
25	34	0.101743
25	35	0.101197
25	36	0.100451
25	37	0.099569
25	38	0.098587
25	39	0.097481
25	40	0.096228
25	41	0.094823
25	42	0.093339
25	43	0.091881
25	44	0.090519
25	45	0.089223
25	46	0.087943
25	47	0.086653
25	48	0.085385
25	49	0.084180
25	50	0.083080
25	51	0.082111
25	52	0.081267
25	53	0.080538
25	54	0.079914
25	55	0.079384
25	56	0.078939
25	57	0.078568
25	58	0.078264
25	59	0.078022
25	60	0.077837
25	61	0.077703
25	62	0.077615
25	63	0.077568
25	64	0.077556
25	65	0.077575
25	66	0.077622
25	67	0.077695
25	68	0.077787
25	69	0.077894
25	70	0.078010
25	71	0.078131
25	72	0.078251
25	73	0.078365
25	74	0.078469
25	75	0.078556
25	76	0.078621
25	77	0.078661
25	78	0.078669
25	79	0.078640
25	80	0.078569
25	81	0.078451
25	82	0.078282
25	83	0.078057
25	84	0.077774
25	85	0.077431
25	86	0.077027
25	87	0.076557
25	88	0.076021
25	89	0.075416
25	90	0.074739

B.7 $C_T(\bar{\delta}_e, \alpha)$

CTHDE
Increment due to elevon at high aoa, low speed.
020119
2
DE
ALFA
-30 -10 0
-30 30 0
-30 31 0.043703
-30 32 0.041115
-30 33 0.038093
-30 34 0.034746
-30 35 0.031210
-30 36 0.027599
-30 37 0.024009
-30 38 0.020514
-30 39 0.017136
-30 40 0.013942
-30 41 0.011021
-30 42 0.008546
-30 43 0.006661
-30 44 0.005365
-30 45 0.004544
-30 46 0.004064
-30 47 0.003815
-30 48 0.003745
-30 49 0.003826
-30 50 0.004068
-30 51 0.004473
-30 52 0.005006
-30 53 0.005633
-30 54 0.006316
-30 55 0.007018
-30 56 0.007704
-30 57 0.008342
-30 58 0.008926
-30 59 0.009459
-30 60 0.009944
-30 61 0.010385
-30 62 0.010784
-30 63 0.011146
-30 64 0.011472
-30 65 0.011767
-30 66 0.012031
-30 67 0.012269
-30 68 0.012481
-30 69 0.012669
-30 70 0.012835
-30 71 0.012982
-30 72 0.013111
-30 73 0.013222
-30 74 0.013310
-30 75 0.013367
-30 76 0.013384
-30 77 0.013354
-30 78 0.013269
-30 79 0.013121
-30 80 0.012906
-30 81 0.012630
-30 82 0.012300
-30 83 0.011926
-30 84 0.011516
-30 85 0.011083
-30 86 0.010636
-30 87 0.010185
-30 88 0.009740
-30 89 0.009312
-30 90 0.008911
-20 -10 0

-20	30	0
-20	31	0.012686
-20	32	0.011195
-20	33	0.009757
-20	34	0.008349
-20	35	0.006909
-20	36	0.005486
-20	37	0.004137
-20	38	0.002896
-20	39	0.001726
-20	40	0.000587
-20	41	-0.000540
-20	42	-0.001595
-20	43	-0.002488
-20	44	-0.003162
-20	45	-0.003662
-20	46	-0.004035
-20	47	-0.004288
-20	48	-0.004367
-20	49	-0.004209
-20	50	-0.003753
-20	51	-0.002949
-20	52	-0.001793
-20	53	-0.000368
-20	54	0.001203
-20	55	0.002793
-20	56	0.004278
-20	57	0.005552
-20	58	0.006608
-20	59	0.007470
-20	60	0.008164
-20	61	0.008714
-20	62	0.009145
-20	63	0.009482
-20	64	0.009745
-20	65	0.009939
-20	66	0.010068
-20	67	0.010137
-20	68	0.010151
-20	69	0.010114
-20	70	0.010030
-20	71	0.009905
-20	72	0.009743
-20	73	0.009547
-20	74	0.009320
-20	75	0.009064
-20	76	0.008778
-20	77	0.008465
-20	78	0.008127
-20	79	0.007763
-20	80	0.007377
-20	81	0.006970
-20	82	0.006550
-20	83	0.006124
-20	84	0.005701
-20	85	0.005291
-20	86	0.004902
-20	87	0.004544
-20	88	0.004225
-20	89	0.003955
-20	90	0.003743
-10	-10	0
-10	30	0
-10	31	-0.002308
-10	32	-0.003319
-10	33	-0.004431
-10	34	-0.005637
-10	35	-0.006967
-10	36	-0.008344
-10	37	-0.009683
-10	38	-0.010923
-10	39	-0.012076
-10	40	-0.013171
-10	41	-0.014232
-10	42	-0.015197
-10	43	-0.015977
-10	44	-0.016520
-10	45	-0.016869
-10	46	-0.017072
-10	47	-0.017152
-10	48	-0.017074
-10	49	-0.016791
-10	50	-0.016260
-10	51	-0.015452
-10	52	-0.014387
-10	53	-0.013094
-10	54	-0.011599
-10	55	-0.009931
-10	56	-0.008132
-10	57	-0.006296
-10	58	-0.004527
-10	59	-0.002925
-10	60	-0.001592
-10	61	-0.000572
-10	62	0.000187
-10	63	0.000749
-10	64	0.001176
-10	65	0.001531
-10	66	0.001882
-10	67	0.002293
-10	68	0.002805
-10	69	0.003391
-10	70	0.004012
-10	71	0.004628
-10	72	0.005202
-10	73	0.005693
-10	74	0.006073
-10	75	0.006355
-10	76	0.006566
-10	77	0.006728
-10	78	0.006867
-10	79	0.007007
-10	80	0.007174
-10	81	0.007382
-10	82	0.007605
-10	83	0.007803
-10	84	0.007938
-10	85	0.007972
-10	86	0.007866
-10	87	0.007582
-10	88	0.007082
-10	89	0.006328
-10	90	0.005281
0	-10	0
0	30	0
0	31	0
0	32	0
0	33	0
0	34	0
0	35	0
0	36	0
0	37	0
0	38	0
0	39	0
0	40	0
0	41	0
0	42	0
0	43	0
0	44	0
0	45	0
0	46	0
0	47	0
0	48	0
0	49	0
0	50	0
0	51	0
0	52	0
0	53	0
0	54	0
0	55	0
0	56	0
0	57	0
0	58	0
0	59	0
0	60	0
0	61	0
0	62	0
0	63	0
0	64	0
0	65	0
0	66	0
0	67	0
0	68	0
0	69	0
0	70	0
0	71	0
0	72	0
0	73	0
0	74	0
0	75	0
0	76	0
0	77	0
0	78	0
0	79	0
0	80	0
0	81	0
0	82	0
0	83	0
0	84	0
0	85	0
0	86	0
0	87	0
0	88	0
0	89	0
0	90	0
10	-10	0
10	30	0
10	31	0.015211
10	32	0.016549
10	33	0.017996
10	34	0.019370
10	35	0.020621
10	36	0.021818
10	37	0.023021
10	38	0.024204
10	39	0.025247
10	40	0.026022
10	41	0.026412
10	42	0.026405
10	43	0.026115
10	44	0.025648
10	45	0.025013
10	46	0.024199
10	47	0.023216
10	48	0.022125
10	49	0.020984
10	50	0.019855
10	51	0.018782
10	52	0.017779
10	53	0.016855
10	54	0.016015
10	55	0.015254
10	56	0.014566
10	57	0.013942
10	58	0.013379
10	59	0.012876
10	60	0.012429
10	61	0.012029
10	62	0.011645
10	63	0.011241
10	64	0.010782
10	65	0.010235
10	66	0.009573
10	67	0.008831
10	68	0.008059
10	69	0.007311
10	70	0.006641
10	71	0.006097
10	72	0.005679
10	73	0.005348
10	74	0.005066
10	75	0.004792
10	76	0.004488
10	77	0.004137
10	78	0.003764
10	79	0.003401
10	80	0.003078
10	81	0.002824
10	82	0.002642
10	83	0.002517
10	84	0.002429
10	85	0.002361
10	86	0.002297

10	87	0.002218
10	88	0.002108
10	89	0.001948
10	90	0.001721
20	-10	0
20	30	0
20	31	0.039485
20	32	0.042480
20	33	0.045127
20	34	0.046797
20	35	0.047547
20	36	0.047586
20	37	0.047136
20	38	0.046385
20	39	0.045381
20	40	0.044095
20	41	0.042513
20	42	0.040703
20	43	0.038762
20	44	0.036750
20	45	0.034631
20	46	0.032372
20	47	0.029996
20	48	0.027581
20	49	0.025219
20	50	0.023000
20	51	0.020999
20	52	0.019258
20	53	0.017773
20	54	0.016508
20	55	0.015422
20	56	0.014479
20	57	0.013639
20	58	0.012869
20	59	0.012134
20	60	0.011408
20	61	0.010692
20	62	0.009995
20	63	0.009324
20	64	0.008688
20	65	0.008096
20	66	0.007559
20	67	0.007082
20	68	0.006664
20	69	0.006302
20	70	0.005994
20	71	0.005738
20	72	0.005532
20	73	0.005373
20	74	0.005259
20	75	0.005189
20	76	0.005154
20	77	0.005144
20	78	0.005143
20	79	0.005140
20	80	0.005121
20	81	0.005073
20	82	0.004982
20	83	0.004838
20	84	0.004629
20	85	0.004346
20	86	0.003978
20	87	0.003515
20	88	0.002946
20	89	0.002261
20	90	0.001450
30	-10	0
30	30	0
30	31	0.069032
30	32	0.070118
30	33	0.070918
30	34	0.071226
30	35	0.070989
30	36	0.070306
30	37	0.069284
30	38	0.068008
30	39	0.066489
30	40	0.064724
30	41	0.062717
30	42	0.060538
30	43	0.058286
30	44	0.056022
30	45	0.053711
30	46	0.051298
30	47	0.048750
30	48	0.046100
30	49	0.043416
30	50	0.040767
30	51	0.038212
30	52	0.035773
30	53	0.033470
30	54	0.031323
30	55	0.029352
30	56	0.027573
30	57	0.025976
30	58	0.024539
30	59	0.023241
30	60	0.022062
30	61	0.020980
30	62	0.019976
30	63	0.019029
30	64	0.018122
30	65	0.017254
30	66	0.016428
30	67	0.015648
30	68	0.014918
30	69	0.014242
30	70	0.013624
30	71	0.013068
30	72	0.012571
30	73	0.012123
30	74	0.011712
30	75	0.011326
30	76	0.010953
30	77	0.010581
30	78	0.010199
30	79	0.009795
30	80	0.009367
30	81	0.008916
30	82	0.008442
30	83	0.007949
30	84	0.007442
30	85	0.006923
30	86	0.006397
30	87	0.005868
30	88	0.005341
30	89	0.004819
30	90	0.004306

C. Block Diagram for ADMIRE Extract & Plot

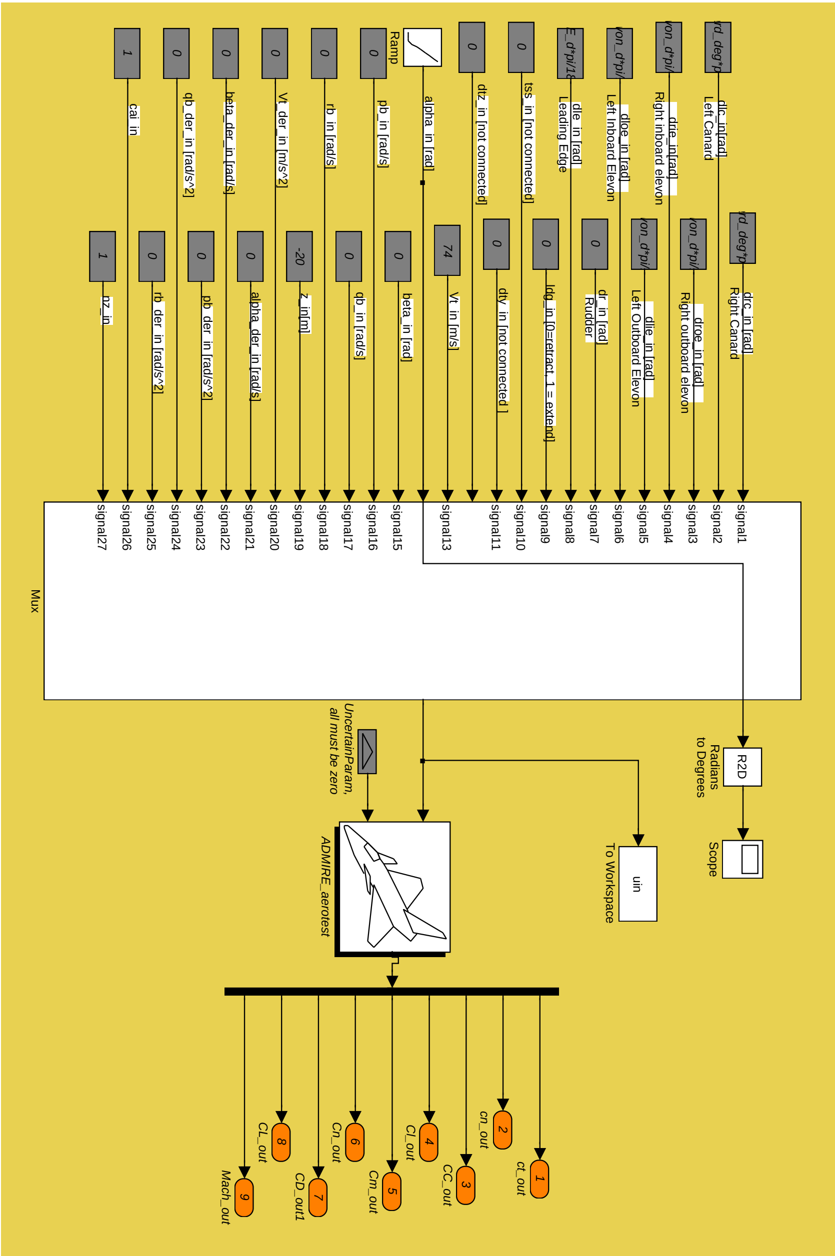

Figure C.1: Simulation model used to extract coefficient from ADMIRE